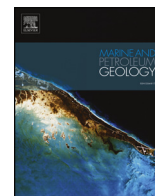




ELSEVIER

Contents lists available at ScienceDirect

## Marine and Petroleum Geology

journal homepage: [www.elsevier.com/locate/marpetgeo](http://www.elsevier.com/locate/marpetgeo)

Research paper

# The hydrocarbon generation potential and migration in an alkaline evaporite basin: The Early Permian Fengcheng Formation in the Junggar Basin, northwestern China

Kuanhong Yu\*, Yingchang Cao, Longwei Qiu, Peipei Sun

School of Geosciences, China University of Petroleum, Qingdao, Shandong, 266580, China



## ARTICLE INFO

## Keywords:

Source rocks

Benthic microbial mats

Algae

Stylolite

Hydrocarbon expulsion and migration

Mahu sag

## ABSTRACT

The Permian Fengcheng Formation in the Mahu Sag in the Junggar Basin represents deposition in a rare alkaline saline lake, with hydrologically closed conditions, alkaline saline brines, and intense volcanic activity. The Fengcheng Formation contains large volumes of high-quality source rocks, which form not only in the depocenter but also in the wide, shallow lake margins. The source rocks analyzed in this study are different from those in most other ancient lakes in the following aspects: genesis and occurrence of organic matter, kerogen type, lithological composition, and hydrocarbon migration pathway. This study showed that the Fengcheng Formation has high hydrocarbon generation potential and that combinations of multiple paths enhanced the hydrocarbon expulsion and migration. Benthic microbial mats and algae that bloomed in the alkaline saline lake represent the dominant types of organic matter. Due to their specific composition, the evaporites may have catalyzed hydrocarbon generation via organic-inorganic interactions, while intergranular seams in bedded/laminated evaporites provided paths for hydrocarbon migration. Stylolites, with high contents of brittle minerals and low clay content, also allowed favorable paths for hydrocarbon expulsion and migration. Combining hydrocarbon expulsion fractures in the organic-rich laminae, fractures and microfractures caused by compressive tectonic stress, pathway networks formed that enhanced the efficiencies of both hydrocarbon expulsion and migration.

## 1. Introduction

High-quality organic-rich deposits form and are preserved under different conditions in lakes; anoxic conditions are especially the best environments (Tänavsuu-Milkevičienė and Sarg, 2012). Alkaline saline lakes are one type of environment for organic-rich deposit preservation (Talbot, 1988), such as the organic-rich oil shales in the Green River Formation (Mercier, 2012; Johnson et al., 2014, 2015; Birdwell et al., 2017), the Qianjiang Formation in the Jiangnan Basin (Yang et al., 1983; Fang, 2002; Chen et al., 2002), the sodium carbonates-bearing oil shales in the Hetaoyuan Formation in the Biyang Depression of the Nanxiang Basin (Wang et al., 1983; Tuo et al., 1997; Ma et al., 2013), and the Wulidui Formation in the Tongbai Basin (Zhou et al., 2006). These evaporite-bearing successions are all rich in organic matter and generated large amounts of hydrocarbons.

The Early Permian Fengcheng Formation is the most important source rock stratum in the Mahu Sag portion of the Junggar Basin in northwestern China and is rich in tight oil resources (Hu et al., 2016,

2017). This formation contains the oldest, highest-quality, alkaline saline lacustrine source rock in the world, and the hydrocarbon potential may be even better than the organic geochemical indices reflect (Cao et al., 2015; Ren et al., 2017). Additionally, recent research has demonstrated that the organic-rich Fengcheng Formation covered a larger area than the Mahu Sag, as it extended to the northwestern Halalate Mountains region; therefore, the hydrocarbon generation potential is much larger than previously recognized (Wang et al., 2014).

The correlations between oils in the overlying reservoirs and the extractable organic matters in the source rocks of the Fengcheng Formation show that most of the oils came from the Fengcheng Formation (Cao et al., 2006; Wang et al., 2014; Huang et al., 2016). Previous research on the Fengcheng Formation has concentrated on the origin of dolomites (Feng et al., 2011; Lu et al., 2012; Zhang et al., 2012; Zhu et al., 2013), the alteration of volcanic sediments (Zhu et al., 2012a,b; Zhu et al., 2016), the volcanic reservoir (Zhu et al., 2012a,b), the tight reservoir (Kuang et al., 2012; Tao et al., 2016), and the evaporites (Jiang et al., 2012; Yu et al., 2016a,b; Wang, 2017). Previous

\* Corresponding author.

E-mail address: [yukuanhong@upc.edu.cn](mailto:yukuanhong@upc.edu.cn) (K. Yu).<https://doi.org/10.1016/j.marpetgeo.2018.08.010>

Received 23 March 2018; Received in revised form 7 August 2018; Accepted 10 August 2018

Available online 11 August 2018

0264-8172/ © 2018 Elsevier Ltd. All rights reserved.

researchers have long recognized that the source rocks in the Early Permian Fengcheng Formation have high hydrocarbon potential. These hydrocarbon source rocks have the following characteristics that make them different from most lacustrine source rocks. ① Fine-grained organic-rich source rock lithofacies alternate with evaporite layers, and various evaporite minerals occur within the source rocks. It is proposed that these evaporite minerals may provide important influences on the evolution of organic matter, hydrocarbon generation, migration and accumulation. ② The Fengcheng Formation was deposited in a hydrologically closed lake, with the organic material mainly produced within the lake, as opposed to extrabasinal material transported into the basin by runoff. ③ The specific composition of the source rocks may be beneficial to hydrocarbon expulsion. ④ The multiple types of micropathways, e.g., intergranular seams in evaporites, stylolites, microfractures, and hydrocarbon expulsion fractures, may combine and elevate the hydrocarbon expulsion efficiency of the source rocks.

This work focuses on the Fengcheng Formation in the Mahu Sag, which contains fine-grained organic-rich source rocks and includes the major types of source rocks, to study the following: ① the occurrences of organic matters, ② the hydrocarbon potential of source rocks, and ③ the factors that control elevated hydrocarbon expulsion efficiency.

## 2. Geological setting

The Junggar Basin is located in the northwestern Xinjiang Uygur Autonomous Region, China, and covers an area of  $1.3 \times 10^5$  km<sup>2</sup>. This basin is a triangular basin that lies at the juncture of three tectonic domains: the Kazakhstan, Siberia, and Tarim cratons (Cao et al., 2006; Chen et al., 2016a,b). To the east are the Kelameili Mountains, to the northwest are the Zaire Mountains and Halalate Mountains, to the north are the Aletay Mountains, and to the south are the Boro Horo Mountains and Bogda Mountains (Fig. 1A). This basin is a renowned superimposed basin characterized by source rocks that were deposited in environments that changed from marine (Carboniferous) to lacustrine (Permian) conditions (Hu et al., 2016, 2017). The studied Mahu Sag is located in the northwestern part of the Junggar Basin and is one of the most prolific oil- and gas-producing areas (Liu et al., 2016).

Most of the faults in the study area are thrust faults and are oriented NE-SW because of multiple stages of compressional tectonic events; these faults include the North Xiahong Fault, North Wulanlingge Fault, South X-1 Fault, etc. (Fig. 1B). A northwestern nappe was formed during the Late Carboniferous-Early Permian due to strong collisional forces (Fig. 1C). Structural inversions uplifted part of the depocenter (wells FN-7 and AK-1), which provides data for studying the evaporite center of the Early Permian Fengcheng Formation (Fig. 1C).

The stratigraphic sequence consists of Carboniferous to recent sediments, and the depositional environment changed from marine during the Carboniferous to non-marine during the Early Permian (Fig. 2A) (Bian et al., 2010; Yu et al., 2016a,b). The lithology of the Carboniferous is dominated by volcanic rocks, pyroclastic rocks, and conglomerates. Gray-green conglomerates, volcanic tuff and pyroclastics occur in the Jiamuhe Formation, and dark mudstone, conglomerates, sandstones, dolomitic tuff and evaporites occur in the Lower Fengcheng Formation (Cao et al., 2006; Xiao et al., 2014; Liu et al., 2016; Chen et al., 2016a,b). During the Early Permian, a marine regression progressed from northwest to southeast, and the northwestern Junggar Basin changed to lake depositional environments that were closed to marine influence (Fig. 2B) (Bian et al., 2010). Volcanic eruptions were frequent, and tectonic activity was intensive, which resulted in the widespread distribution of volcanic and pyroclastic rocks (Zhu et al., 2012a,b; Zhu et al., 2016; Yu et al., 2016a,b). Additionally, Mahu Lake is a typical alkaline saline lake in which evaporites form in the hydrologically closed to semi-closed basinal area. Brines have the highest salinity during Middle Fengcheng Formation deposition, and then they freshen gradually during Upper Fengcheng Formation deposition (Fig. 2A). The evaporites in the Fengcheng Formation are

dominated by sodium carbonates, the composition of which is controlled by the specific solutes in the brine when the Fengcheng Formation was deposited (Yu et al., 2016a,b). The alkaline saline environment formed high-quality organic-rich source rocks, which generated abundant hydrocarbon resources for the overlying reservoir (Cao et al., 2015; Hu et al., 2017; Ren et al., 2017).

## 3. Datasets and methodology

This study was based on data from core observations, microscopy characterizations, and geochemical analyses provided by the Xinjiang Oilfield Company, China National Petroleum Corporation (CNPC). Core sections totaling 165 m and 626 thin sections from 27 wells were observed. The core sections covered the typical lithology and lithofacies, which can reflect the main depositional environments in the Early Permian deposits of the Mahu Lake. Based on the core and thin section observations, the extent of organic-rich source rocks was evaluated, and the occurrences of organic matter in source rocks and of paths for hydrocarbon expulsion and migration were characterized in detail under the microscope. Additionally, 46 sets of geochemical data were collected from the source rocks, namely, 38 pyrolysis analyses, 38 total organic carbon (TOC) measurements, and 17 sets of vitrinite reflectance (VR) testing data (Table 1), and 14 X-Ray Diffraction (XRD) analyses were carried out to characterize the rock compositions. Micro X-Ray Fluorescence (micro-XRF) were used to characterize the elemental composition of source rock lithofacies, which assisted in reflecting the mineral composition and depositional environments.

The TOC content was determined using a LECO CS-400 analyzer, and the Rock-Eval pyrolysis was performed using a Rock-Eval II instrument. The Ro was determined using an oil immersion lens and a Leica MPV Compact II reflected light microscope fitted with a microphotometer. The reflectance for each sample was calculated by averaging the histogram of reliable data. The bitumen content and gross composition analysis were determined by conventional Soxhlet extraction methods. The XRD analysis was carried out using powdered bulk rock materials in a Dmax 12KW powder X-ray diffractometer, using Fe-filtered Co K $\alpha$  radiation.

The Micro-XRF images were collected using a M4 TORNADO made by BRUKER, a sophisticated piece of equipment that employs a useful method for highly sensitive and a non-destructive elemental analysis of diverse samples. Such diverse sample types include inhomogeneous and irregularly shaped specimens in addition to thin sections without cover slips. In this study, major elements of some uncovered thin sections were detected, with the X-ray tube set at parameters of 20 mbar, 50 kv and 600  $\mu$ A. The sample databases were analyzed and depicted by M4 TORNADO software, and the content of major elements was revealed in different colors in the panel, in which the relative abundances of rock-forming elements can be easily observed.

## 4. Characteristics of organic-rich source rocks

### 4.1. An overview of the distribution of organic-rich source rocks

To detect the extent of organic-rich source rocks and to characterize the source rocks in each depositional subenvironment, four typical wells along a NE-SW line were selected and studied in detail (Fig. 3). A wide low-gradient lake margin occurred to the northeast, and a depocenter was located to the southwest. A slope (transitional zone) developed between the shallow lake margin and the depocenter. Additionally, according to the current drilling data and the planar seismic attributes in the study area, volcanic eruptions and magmatic activity mainly occurred to the northeast (the area with well labels "X-") (Zhu et al., 2012a,b), with volcanic eruptions providing abundant ashes and dusts. The content of volcanic sediments is very high in all the fine-grained source rocks analyzed. The sediments within the selected wells represent different depositional environments, and the source rocks in

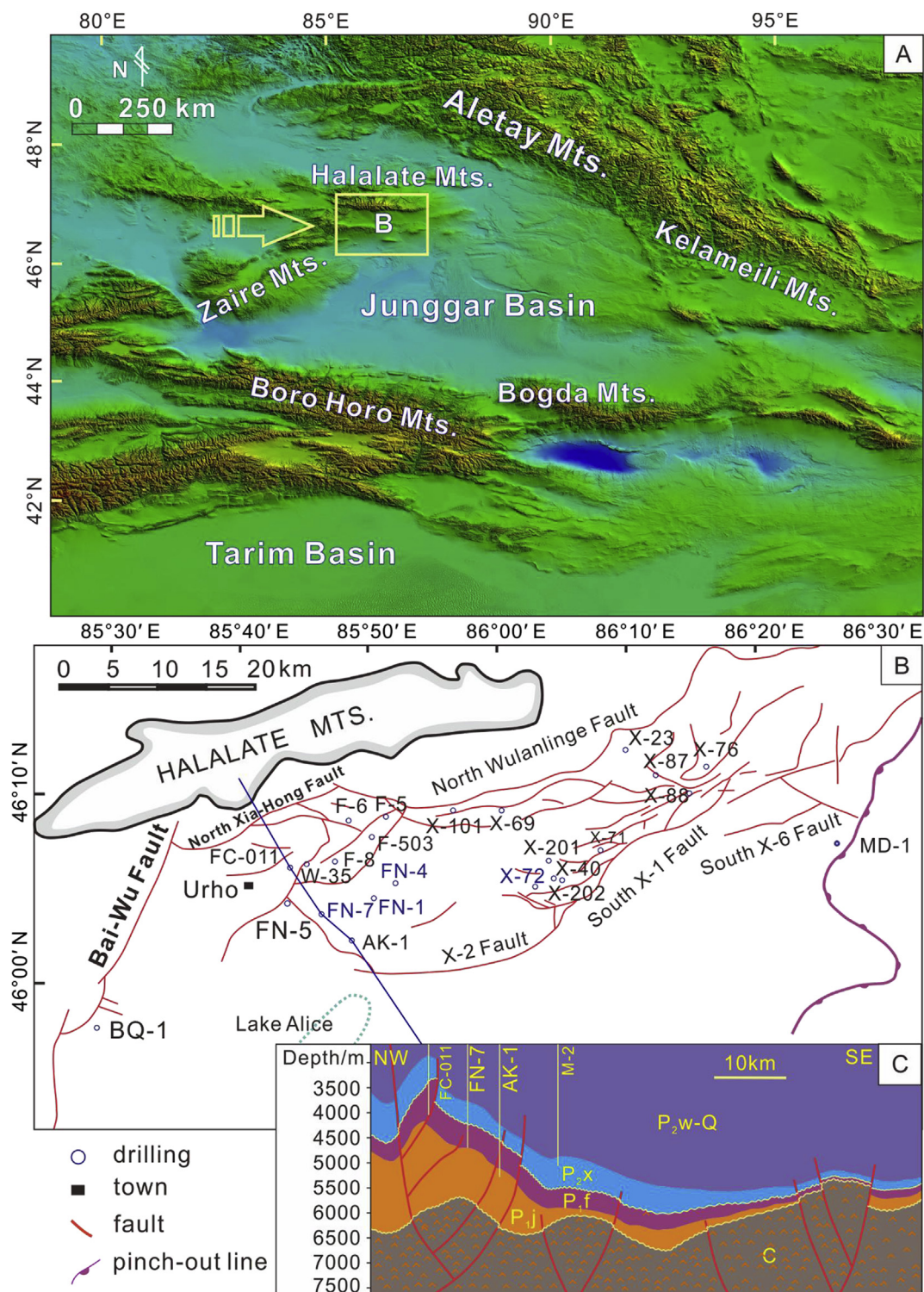


**Fig. 1.** Locality and generalized geologic map of the Mahu Sag, Junggar Basin in China. (A) Location of the Junggar Basin and the Mahu Sag. The Mahu Sag is located at the northwestern Junggar Basin. (B) Sketch of the Mahu Sag and main drillings and faults. The Mahu Sag was a foreland basin controlled by NNE-SSW boundary thrust faults. (C) NW-SE tectonic profile across the Mhuhu Sag.

these wells reveal variable characteristics.

Wells AK-1 and FN-7 are located near the depocenter of the Mahu Sag, where thick, fine-grained organic-rich source rocks developed. The source rocks in the middle part of the Fengcheng Formation in these two wells are characterized by bedded, light-colored sodium carbonates, which alternate with dark-colored, fine-grained tuff/tuffaceous, organic-rich source rocks (Yu et al., 2016a,b). The abundance of sodium

carbonates can be easily identified from well logs by the high resistivities on the resistivity curves (RT) (Fig. 3). The detailed characteristics of layered organic-rich source rocks in AK-1 and FN-7 are presented in Figs. 4 and 5.

Well FN-1 is located in the transitional zone between the depocenter and the shallow lake margin. There are no bedded evaporites in the Fengcheng Formation in well FN-1, although an abundance of

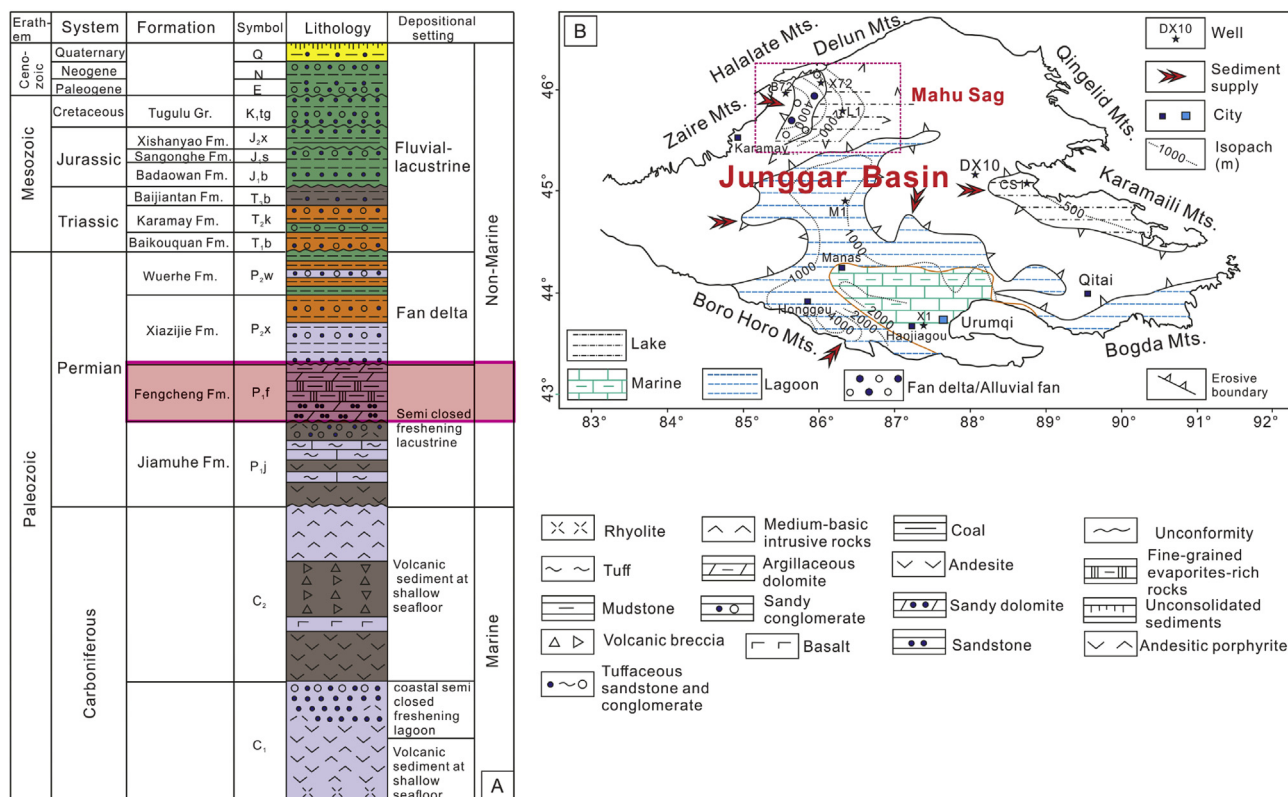


Fig. 2. Stratigraphic column in the northwestern Junggar Basin and lithofacies paleogeography in the Permian Junggar Basin. (A) Generalized stratigraphic sequence of the study area (modified after (Cao et al., 2005; Xiao et al., 2014; Shi et al., 2015; Ma et al., 2015). (B) Lithofacies paleogeography in the Permian Junggar Basin. The Mahu Sag was a lake near the sea formed by the southeast sea regression (Bian et al., 2010).

diagenetic authigenic saline minerals are present. Tuffs and volcanic rocks exist in this well, and magmatic-related hydrothermal activities, such as hot springs, are suggested from the attributes of the core of FN-1.

Well FN-4 is located in the northeastern part of the study area, a region which represents a shallow lake margin depositional environment. The residual thickness of the Fengcheng Formation is approximately 500 m, and the lithology is dominated by volcanic rocks, pyroclastic rocks, dolomitic tuffs, and tuffaceous rocks. The fine-grained lithology, however, is dominated by tuffs and tuffaceous rocks, in which most of the organic matter occurs. There are but few evaporite minerals in this well.

Based on an integrated analysis of the lithofacies, sedimentary thickness and resistivity well logs from four representative wells, the distribution of source rocks can be summarized as follows: (1) The depocenter is located in the southwestern part of the study area and developed very thick and voluminous organic-rich source rocks. (2) Fine-grained organic-rich source rocks occur associated with evaporites or authigenic saline minerals.

#### 4.2. Lithological characteristics of source rocks in the depocenter

Well AK-1 is located near the depocenter and contains very thick, fine-grained organic-rich source rocks. Core scanning images of the lower part of the Fengcheng Formation in well AK-1 are characterized by repeated dark-colored organic-rich laminae and light-colored evaporite laminae couplets (Fig. 4). Although the laminae are deformed, the contacts between organic-rich laminae and evaporite laminae can be recognized easily (lower part of Fig. 4A). The single lithological laminae thickness is only on the order of a few millimeters, and both the organic-rich laminae and evaporitic laminae are easily separated or crinkled by deformation (upper part of Fig. 4A). The dark-colored

portions contain high amounts of organic matter and kerogen. In some parts of the core scanning images, a few deformities are noted, and the organic-rich laminae and evaporite couplets maintain extensive horizons (Fig. 4B). In the close-up view of the upper left corner, we can observe the relationship between the light-colored evaporite laminae and the dark-colored organic-rich laminae. The contact interfaces between different laminae are clearly distinguishable and trend horizontal to subhorizontal (Fig. 4C). Additionally, no coarse-grained textures can be found in the dark-colored organic-rich laminae.

Well FN-7 is located in the lower part of the slope to the depocenter, and the petrographic compositions and stratigraphic sequence of the Fengcheng Formation are similar to those in well AK-1. The lithological columns of wells AK-1 and FN-7 have developed very thick layers of fine-grained organic-rich source rocks in the Fengcheng Formation. The well log characteristics of both wells are also similar with high amplitudes for the resistivity curves (RT) in the middle Fengcheng Formation (Fig. 3). There are no drilling cores from the middle Fengcheng Formation in well AK-1, and fortunately, we obtained typical bedded sodium carbonates-bearing successions in the middle Fengcheng Formation in the well FN-7. Because of comparable well log curves between wells AK-1 and FN-7, it can be assumed that they have similar lithological compositions and lithofacies. As a result, the characteristics of the core sections in the middle Fengcheng Formation from well FN-7 can represent those that formed in the depocenter of this evaporite basin. For the same reason, the characteristics of the core section in the lower Fengcheng Formation from well AK-1 can represent those of the lower Fengcheng Formation in the whole depocenter.

The typical core succession in the middle Fengcheng Formation is characterized by bedded sodium carbonates successions. Lithologically, the core is composed of two repeated, distinctly coupled lithofacies layers: light-colored sodium carbonates layers and dark-colored, fine-grained organic-rich tuffaceous layers (Fig. 5A). Organic matter has

**Table 1**  
Source rock sample data of the Fengcheng Formation.

Sample NO.	Well No.	Strata	Depth (m)	Rock-Eval pyrolysis data			TOC (%)	HI (mg/g)	Ro (%)
				S1 (mg/g)	S2 (mg/g)	Tmax (°C)			
1	FN-1	P <sub>1</sub> f <sub>3</sub>	4092	0.14	3.25	443	1.54	211	/
2	FN-1	P <sub>1</sub> f <sub>3</sub>	4095.17	1.6	5.84	435	1.46	400	/
3	FN-1	P <sub>1</sub> f <sub>3</sub>	4096.2	0.24	1.77	435	0.69	257	/
4	FN-1	P <sub>1</sub> f <sub>3</sub>	4096.48	0.56	6.42	436	1.22	526	/
5	FN-1	P <sub>1</sub> f <sub>3</sub>	4110	0.16	1.13	450	0.7	161	/
6	FN-1	P <sub>1</sub> f <sub>3</sub>	4123.27	0.67	6.94	444	1.57	442	/
7	FN-1	P <sub>1</sub> f <sub>3</sub>	4148	0.47	8.36	446	1.63	513	/
8	FN-1	P <sub>1</sub> f <sub>3</sub>	4170	0.66	5.87	438	1.74	337	/
9	FN-1	P <sub>1</sub> f <sub>2</sub>	4181.16	1.05	1.63	436	0.61	267	/
10	FN-1	P <sub>1</sub> f <sub>2</sub>	4188	1.3	6.47	435	1.38	469	/
11	FN-1	P <sub>1</sub> f <sub>2</sub>	4193.27	0.6	1.26	431	0.52	242	/
12	FN-1	P <sub>1</sub> f <sub>2</sub>	4194.27	6.42	5.8	428	1.27	457	/
13	FN-1	P <sub>1</sub> f <sub>2</sub>	4195.31	1.3	2.62	433	0.86	305	3.47
14	FN-1	P <sub>1</sub> f <sub>2</sub>	4196.72	1.43	2.78	435	0.81	343	/
15	FN-1	P <sub>1</sub> f <sub>2</sub>	4231.8	1.07	1.73	433	0.62	279	/
16	FN-1	P <sub>1</sub> f	4233.17*	0.76	3.08	415	0.98	314	3.43
17	FN-1	P <sub>1</sub> f <sub>2</sub>	4320.87	0.15	0.55	440	0.48	115	/
18	FN-1	P <sub>1</sub> f <sub>2</sub>	4326.07	0.13	2.21	434	0.91	243	/
19	FN-1	P <sub>1</sub> f <sub>2</sub>	4336.96	0.62	2.74	440	0.88	311	/
20	FN-1	P <sub>1</sub> f <sub>2</sub>	4338.9	0.69	2.41	429	0.72	335	/
21	FN-1	P <sub>1</sub> f <sub>2</sub>	4357.51	0.74	4.23	437	1.12	378	/
22	FN-1	P <sub>1</sub> f <sub>2</sub>	4369.43	0.5	2.07	432	0.67	309	/
23	FN-1	P <sub>1</sub> f <sub>1</sub>	4444.16	2.4	4.2	430	0.9	467	/
24	FN-1	P <sub>1</sub> f <sub>1</sub>	4444.26	0.11	0.85	450	0.46	185	/
25	F-5	P <sub>1</sub> f <sub>3</sub>	3190.37	0.53	5.27	430	1.25	422	0.67
26	F-5	P <sub>1</sub> f	3209.6*	0.48	9.28	432	2.05	453	0.73
27	F-5	P <sub>1</sub> f <sub>2</sub>	3214.41	0.34	2.58	437	0.77	335	0.59
28	F-5	P <sub>1</sub> f <sub>2</sub>	3221.41	0.52	25.12	432	4.01	626	/
29	F-5	P <sub>1</sub> f <sub>2</sub>	3231.45	0.59	8.32	433	2.72	306	0.6

Sample NO.	Well No.	Strata	Depth (m)	Rock-Eval pyrolysis data			TOC (%)	HI (mg/g)	Ro (%)
				S1 (mg/g)	S2 (mg/g)	Tmax (°C)			
30	F-6	P <sub>1</sub> f	3350*	0.05	0.04	444	0.14	29	/
31	F-7	P <sub>1</sub> f	3186.39*	0.36	4.3	435	1.64	262	1.36
32	F-7	P <sub>1</sub> f	3314.75	/	/	/	/	/	0.66
33	F-7	P <sub>1</sub> f	3363.7	/	/	/	/	/	0.65
34	FN-2	P <sub>1</sub> f	4037.84	/	/	/	/	/	0.9
35	FN-2	P <sub>1</sub> f	4040.85	/	/	/	/	/	0.57
36	FN-2	P <sub>1</sub> f	4063.44*	1.24	4.82	437	1.3	371	0.78
37	FN-2	P <sub>1</sub> f	4099.58	/	/	/	/	/	0.87
38	FN-3	P <sub>1</sub> f	3909.36*	0.16	0.12	391	0.52	23	3.4
39	FN-4	P <sub>1</sub> f	4235.39*	0.18	0.26	442	0.36	72	/
40	FN-5	P <sub>1</sub> f	4070.74*	2.53	1.7	411	0.79	215	/
41	FN-7	P <sub>1</sub> f	4575.96*	3.64	2.61	420	1.25	209	/
42	FN-8	P <sub>1</sub> f	3565.27*	0.9	4.34	440	1.27	342	/
43	FC-1	P <sub>1</sub> f	4274.9*	2.25	1.25	418	0.67	187	/
44	X-88	P <sub>1</sub> f	3660.12	/	/	/	/	/	0.71
45	X-202	P <sub>1</sub> f	4627.46	/	/	/	/	/	1.17
46	X-76	P <sub>1</sub> f	3586.29	/	/	/	/	/	0.58

The data labeled \* are cited from the references (Hu et al., 2016), the other data were collected from Exploration and Development Institute in Xinjiang Oilfield.

accumulated in the dark-colored tuffaceous layers, and salt minerals are scattered within this layer as well. The salt mineralogy is dominated by shortite (Na<sub>2</sub>Ca<sub>2</sub>(CO<sub>3</sub>)<sub>3</sub>) (Yu et al., 2016a,b), which occurs as sub-angular nodules or randomly oriented euhedral crystals in a laminated, tuffaceous matrix (Fig. 5B). Thin section photomicrographs show that a few host sediment inclusions occur in some shortite crystals and that most of these crystals crosscut sedimentary laminae; in addition, some host sediment laminae are deformed as a result of compaction around shortite crystals (Fig. 5C). The organic matter-rich laminae are generally black under the microscope and occur in continuous layers, which are coupled with felsic laminae (Fig. 5D–E). The well-preserved continuous organic-rich laminae reflect a quiescent and anoxic environment.

#### 4.3. Lithological characteristics of source rocks in the transitional zone

Well FN-1 is located in the upper part of the slope to the low-gradient shallow lake margins, with microbial mats readily observed under the microscope (Fig. 6). The microbial mats represent high-quality organic materials both in lacustrine and marine source rocks (Schieber et al., 2007; Olcott and Cestari, 2015; Luo et al., 2016). The microbial mat-bearing source rock in this well consists of two fundamental lithological units: microbial mat-rich laminae (MM) and tuff/tuffaceous sediment-rich laminae (Tuff) (Fig. 6A). These two lithological units alternate frequently. Microbial mats also exist in the tuff/tuffaceous sediment-rich laminae, although they were not abundant as those in the microbial mat laminae, and are discontinuous, while the content of felsic rock-forming minerals increase. From the mosaic view as observed under the optical microscope, we can clearly discern various laminae. The microbial mats in microbial mat-rich laminae are

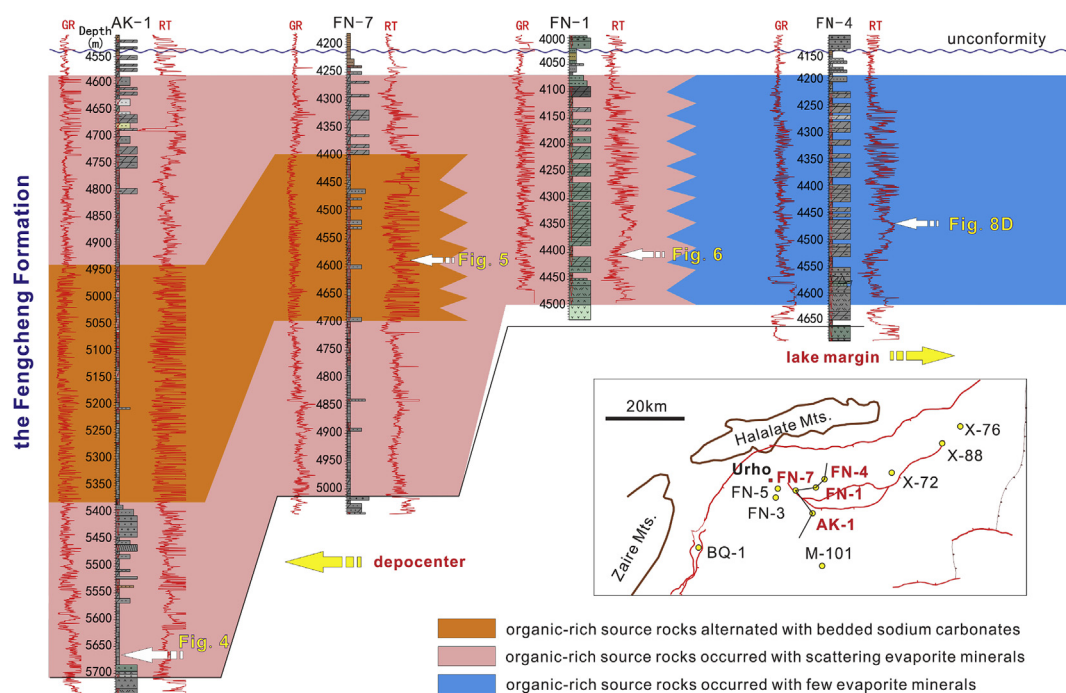


**Fig. 3.** NE-SE transect from the lake margin to the center and the thrust fault zone of the Mahu Sag. To the northeast is the wide low-gradient lake margin, and to the southwest is the deponenter. Source rocks in the deponenter occurred alternating with bedded sodium carbonates, and source rocks also occurred in the shallow lake margins along with the evaporite minerals decrease.

continuous, while those in tuff/tuffaceous sediment-rich laminae are discontinuous. The colors in laminae containing continuous microbial mats are darker than those in laminae with discontinuous microbial mats. Fenestral fabrics are also observed in laminae with continuous microbial mats (Fig. 6B). The combination of major elements S and Fe in the micro-XRF generally reflects pyrite, and this image shows multiple pyrite crystals scattered within the microbial mats (Fig. 6C). The combination of major elements Mg and Ca in the micro-XRF generally suggests dolomite. Based on the element Fe and the blue color dyed by alizarin red S, it can be concluded that Fe-rich (ferroan) dolomites occur in association with the microbial mats (Fig. 6D). The elements Mg, Al, Si, K, Ca in the micro-XRF image can reflect the distributions of carbonates and felsic minerals. As noted previously, the combination of elements Mg and Ca represent dolomite, while the combination of Al, Si, K, Ca then represent felsic minerals. The Fe-rich dolomites are featured with microbial mats, while the felsic minerals are related to tuff/tuffaceous sediments deposition. This image shows that there are no clear boundaries between microbial mat laminae and tuff/tuffaceous sediment-rich laminae. The content of microbial mats decreases with an increase in tuff/tuffaceous sediments, and we can presume that the content of microbial mats would dominate if the supply of tuff/tuffaceous sediments was minimal (Fig. 6E).

Well W-35 is located in the transitional zone, and typical lithofacies are composed of coupled dark-colored organic-rich laminae and light-colored organic-poor laminae (Fig. 7). The light-colored laminae are composed of crystal tuff, and the fine-grained sediments were derived from volcanic eruptions. The tuffs have a low clay content, and laminated interfaces are subhorizontal. Microbial mats are found assembled at the surfaces of tuff layers and reveal darker colors in the laminated interfaces. Microbial mats are assembled in some laminae and resulted in high-quality source rocks (Fig. 7A). The element Ba in the micro-XRF varies with lithological changes (Fig. 7A); compared to tuff laminae, the organic matter (OM)-rich laminae have obviously high Ba content.

#### 4.4. Lithological characteristics of source rocks in shallow lake margins

Wells F-21, X-88, FC-011 and FN-4 are much closer to the shore of the ancient Mahu Lake in the shallow lake margins, and are far from the lake deponenter. The microscopy of polished sections reveals lamalginites as the predominant organic matter in the shallow lake margins (Fig. 8), which can be easily identified by strong yellow fluorescing characteristics (Suárez-Ruiz et al., 2012a,b; Luo et al., 2017). Continuous, planar lamination suggests low-energy depositional conditions, and wavy lamination (Fig. 8A–D) may be caused by uneven surface sediments (Abouelresh and Slatt, 2012; Ma et al., 2016a,b). Alternations of lamalginite-rich laminae and lamalginite-poor laminae typically reflect sedimentological responses to seasonal forcings on water salinity, organic productivity, and runoff in a lake catchment. Algal blooms are common in warm seasons, and organic productivity is high, while fine-grained felsic particles are abundant in lamalginite-poor laminae and may have been formed during relatively cold seasons.

#### 4.5. Geochemical characteristics of the source rocks

The hydrocarbon generation ability depends on the amount of organic matter in the source rocks, and the index parameters to evaluate the hydrocarbon generation ability include the TOC, Rock-Eval pyrolysis data ( $S_1$  and  $S_2$ ), maximum pyrolysis peak temperatures ( $T_{max}$ ), hydrogen index (HI), and vitrinite reflectance of the kerogen (VR). Previous study (Hu et al., 2016) show that the source rocks in the Fengcheng Formation are mainly fair-good source rocks based on the indices TOC and  $S_1 + S_2$  compared to the source rock evaluation standards (Huang et al., 1984).

Different kerogens have different hydrocarbon generation potential, and the identification of the kerogen types is one of the significant items for evaluating source rocks. Rock-Eval pyrolysis data provide a common index to determine the kerogen types. In this study, a plot of HI versus pyrolysis-based  $T_{max}$  is used to classify kerogen types and maturity. The results show that the analyzed samples generally plot in the zone of type II<sub>1</sub> kerogen (Fig. 9A). In Fig. 9A, three samples were not included

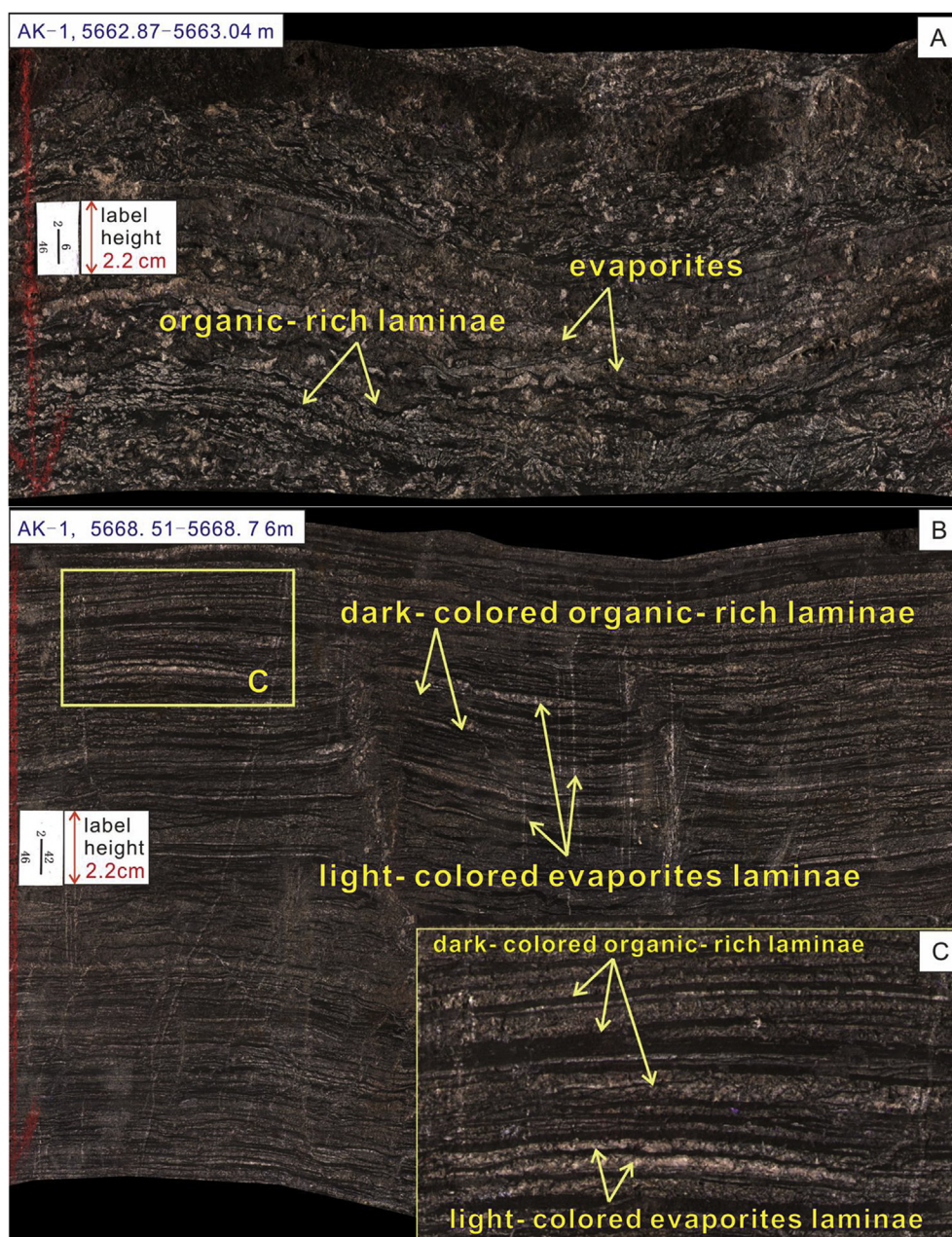


**Fig. 4.** Views of drilling core representing the Lower Fengcheng Formation in the depocenter. (A) Laminated dark-colored source rocks coupled with light-colored evaporites laminae repeatedly, and the laminae deformed, well AK-1, 5662.87–5663.04, (B) Few deformations occurred and the organic-rich laminae and evaporites couples kept extensive horizons, well AK-1, 5668.51–5668.76 m, (C) Zooming characteristics of organic-rich source rock laminae and evaporites laminae couple.

(FN-1, 4195.31 m; FN-1, 4233.17 m; FN-3, 3909.36 m) because their  $R_o$  values were anomalously high ( $> 3.0$ ) and thus were deemed not suitable for kerogen type identification.

$T_{max}$  and VR are common indices used to evaluate source rock thermal maturity (Peters et al., 2005). The equivalent  $T_{max}$  hydrocarbon generation thresholds include the top of the oil window at  $T_{max}$  430 °C and 435 °C and gas/condensate thresholds at 455 °C and 470 °C, respectively, for Type II kerogen. The frequency map of  $T_{max}$  reveals that most source rock samples plot in the mature oil window (Fig. 9B). All the  $T_{max}$  values from Rock-Eval pyrolysis are less than 450 °C (Table 1). The critical thermal maturities of oil and gas generation vary between  $VR = 0.5$ – $1.0\%$  and  $VR = 1.4$ – $3.5\%$ , with different organic matter types (Tissot and Welte, 1984a). The vitrinite reflectance analysis shows that most VR data from 17 samples cluster from 0.5 to 1.0% and there are three abnormally high  $R_o$  values greater than 3%. (Fig. 10

A). The three samples with abnormally high  $R_o$  values may have been affected by magmatic-related hydrothermal activity, and evidence of magmatic influence can be easily observed by the presence of volcanically derived sediments and hydrothermal-related microbial mats in the core sections of well FN-1. Most of the HI values are larger than 250 mg/g, and the majority of the TOC values are larger than 0.5%, which together suggest that most of the source rocks in the Fengcheng Formation retain a good hydrocarbon generating potential (Fig. 10B–C). Additionally, the source rock indices  $R_o$ , HI, and TOC do not vary in an obvious relationship to the burial depths (Fig. 10). Based on the comparisons of source rock evaluation indices in different strata, previous studies have also revealed that source rocks in the Fengcheng Formation remain the most important strata for hydrocarbon generation, compared to both the underlying Permian Jiamuhe Formation and the overlying Wuerhe Formation (Cao et al., 2015).

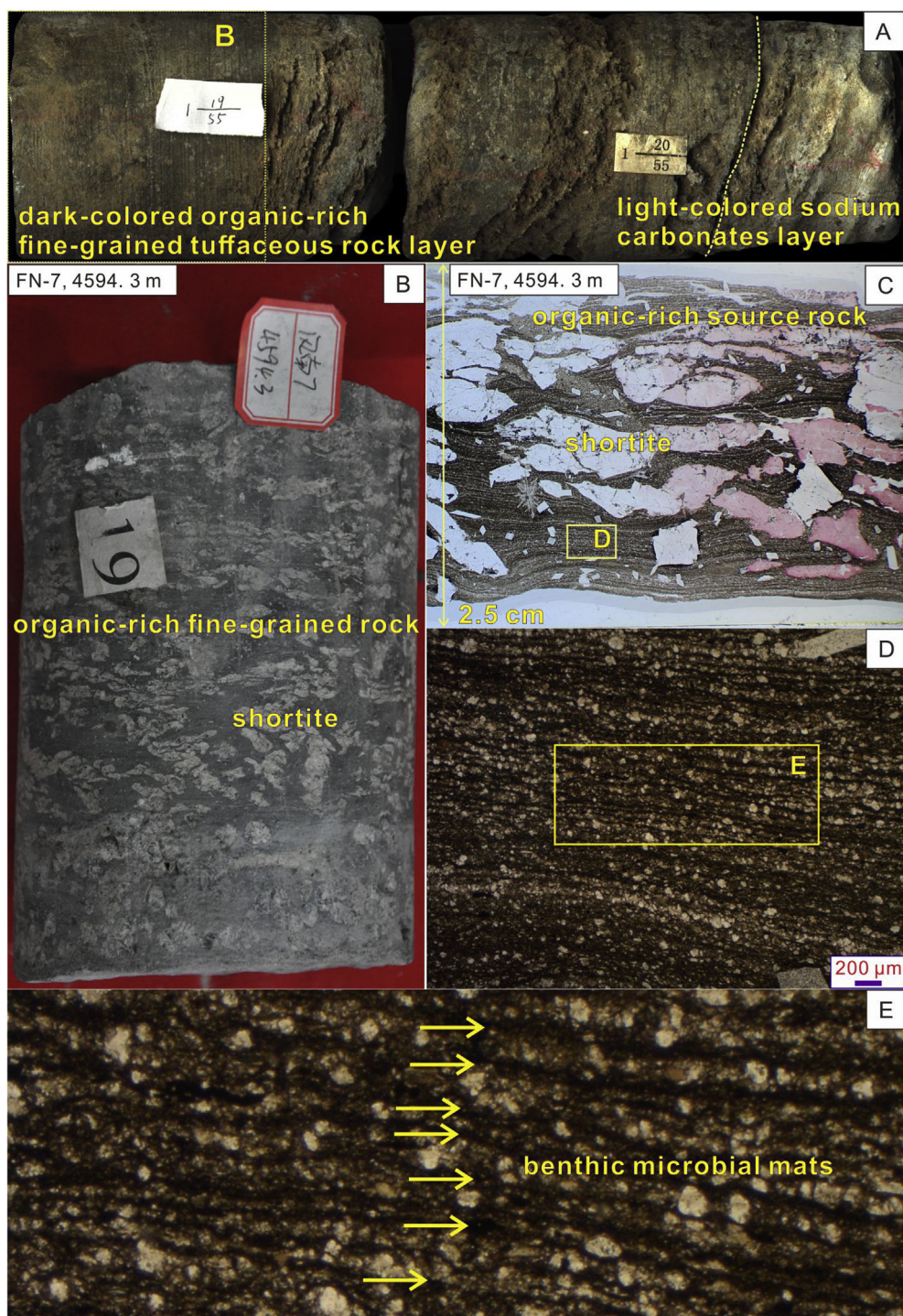


**Fig. 5.** Views of drilling core representing the middle Fengcheng Formation in the depocenter. (A) Core scanning image of alternating bedded light-colored sodium carbonates and dark-colored organic-rich source rock layers, well FN-7, (B) Evaporites, shortite scattered in the organic-rich source rock, well FN-7, 4594.3 m, (C) Photograph of thin section. Shortite scattered in the laminated organic-rich source rocks, well FN-7, 4594.3 m, (D) Characteristics of laminated benthic microbial mats and fine-grained felsic sediments, well FN-7, 4594.3 m, (E) Zooming characteristics of benthic microbial mats under microscope, well FN-7, 4594.3 m.

#### 4.6. Mineral compositions of source rocks

Taking the XRD data from the Fengcheng Formation in well FN-1 as an example, the XRD analyses are illustrated in Fig. 11, and the results indicate that the Fengcheng Formation organic-rich succession consists of clay minerals (avg. 3 wt%), dolomite (avg. 20 wt%), plagioclase (avg. 16 wt%), quartz (avg. 22 wt%), calcite (avg. 11 wt%), ferrodolomite (avg. 2 wt%), K-feldspar (avg. 13 wt%), pyrite (avg. 3 wt%),

reedmergerite (avg. 7 wt%), hornblende (avg. 1 wt%), and some other uncounted components with low contents, such as gypsum, clinoptilolite, and searlesite. Overall, the content of clay minerals is very low, and brittle minerals have high contents. The mineral compositions show significant vertical variations, and the content of carbonates (calcite, dolomite, and ferrodolomite) and other minerals (quartz, plagioclase, K-feldspar, and pyrite) vary in opposite ways.

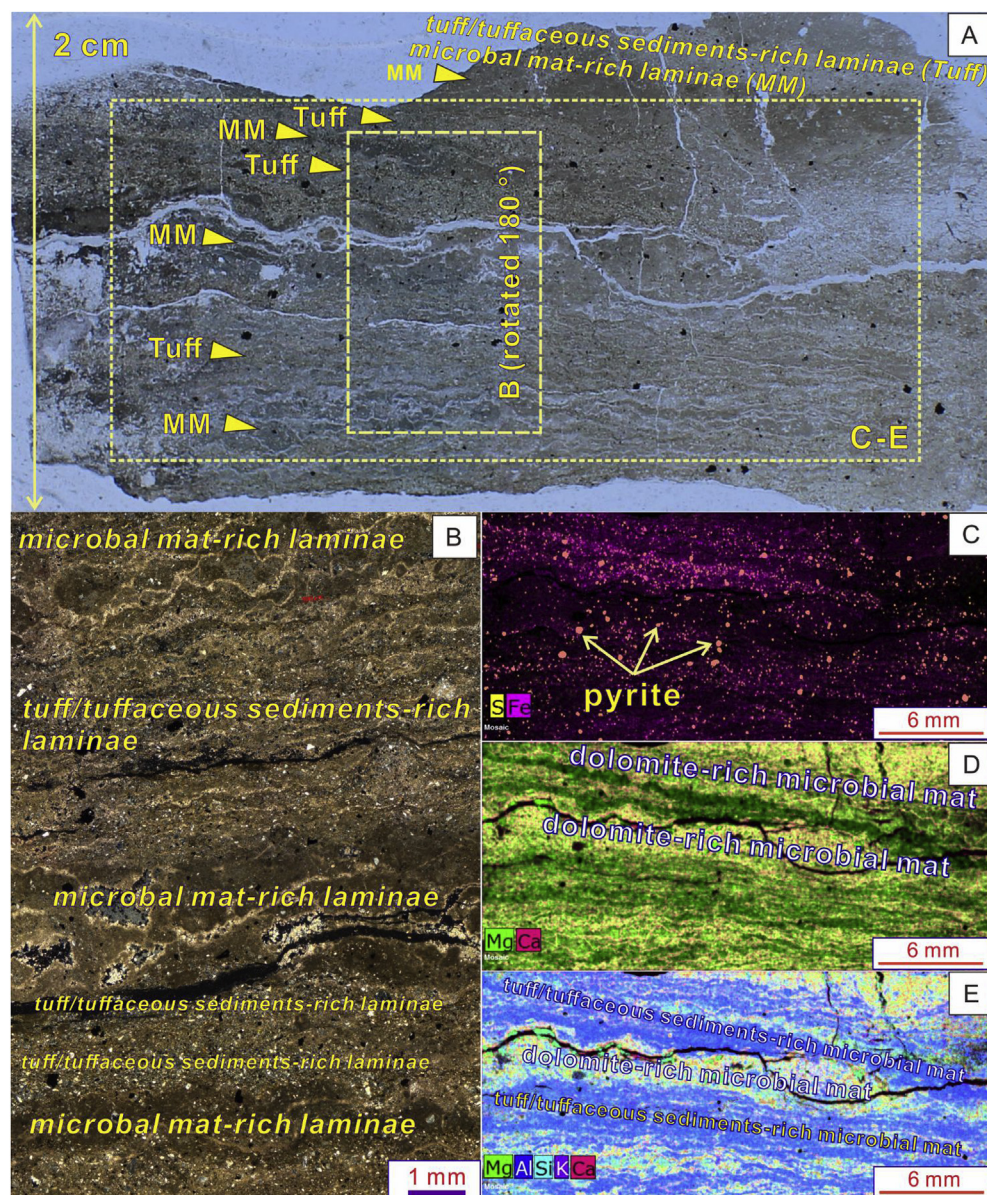


**Fig. 6.** Views of representative microbial mats from shallow lake margins (well FN-1, 4444.41 m). (A) Photograph of thin section of microbial mat-associated source rock. Wavy-crickly microbial mats can be easily identified from the thin section, and Fe-rich dolomite occurred in association with microbial mats. Two fundamental lithological units can be identified: microbial mat-rich laminae (MM) and tuff/tuffaceous sediment-rich laminae (Tuff). These two lithological units alternated repeatedly. (B) Microbial mat-rich laminae alternated with microbial mat-poor laminae, and microbial laminae are continuous in the microbial mat-rich portions, while the microbial mats exist and show discontinuities in the tuff/tuffaceous sediment-rich laminae. (C) Major elements S and Fe in the micro-XRF image. Pyrite can be recognized by the combination of major elements S and Fe. (D) Major elements Mg and Ca in the micro-XRF image. The combination of these two elements generally indicates the distribution of dolomite. These dolomites occurred along with microbial mats. (E) Major elements Mg, Ca, Al, Si and K in the micro-XRF image. This shows the distribution of dolomite and microbial mat-rich lithological units and tuff/tuffaceous sediment-rich lithological units.

## 5. Hydrocarbon expulsion and migration paths

### 5.1. Intergranular seams in sodium carbonates layers

In the above discussion, we note that great sedimentary thicknesses of sodium carbonates-bearing successions occur in the depocenter in the middle Fengcheng Formation. This succession consists of dozens of centimeters of alternating light-colored sodium carbonates layers and dark-colored fine-grained organic-rich source rock layers (Fig. 5). The detailed lithological characteristics of the dark-colored organic-rich layers from core samples and thin sections under the microscope are shown in Fig. 5. Fig. 12 shows representative sedimentary features of light-colored sodium carbonates layers coupled with the dark-colored layers as illustrated in Fig. 5. Thin section photomicrographs show the following: ① The mineral compositions in the light-colored sodium carbonates layers are very complex. Not only large, well-crystallized sodium carbonates (Fig. 12A–C) occur in this layer but also some other minerals and organic matter associated with sodium carbonates, such as shortite and reedmergnerite (Fig. 12D–E). ② The richness of organic matter is not restricted only to the dark-colored layers; organic matter is also enriched in light-colored sodium carbonates layers. In Fig. 12A, the

bottom of the thin section contains abundant organic matter. ③ Intergranular seams in crystalline sodium carbonates are completely filled by yellowish-brown hydrocarbons (Fig. 12A–C), and these seams are favorable paths for hydrocarbon migration because they are unfilled before the hydrocarbons migrate in. The seams in crystalline sodium carbonates are commonly straight, which is beneficial for hydrocarbon migration.

### 5.2. Stylolites

Generally, stylolites are recognized as irregular planes of discontinuity between two lithofacies units, and the two units appear to be interlocked or mutually interpenetrating along a very uneven surface (Park and Schot, 1968). The classifications of stylolites are usually based on the geometry of the stylolites and on their relationship to the bedding plane (Park and Schot, 1968; Koehn et al., 2007, 2016; Norman, 2015). The fundamental control factors on the formation of stylolites are depositional processes and stress-induced dissolutions (Ebner et al., 2009), and the results can be called sedimentary stylolites and tectonic stylolites, respectively (Ben-Itzhak et al., 2014). Stylolites commonly occur in the carbonate stratigraphy. However, in this case,

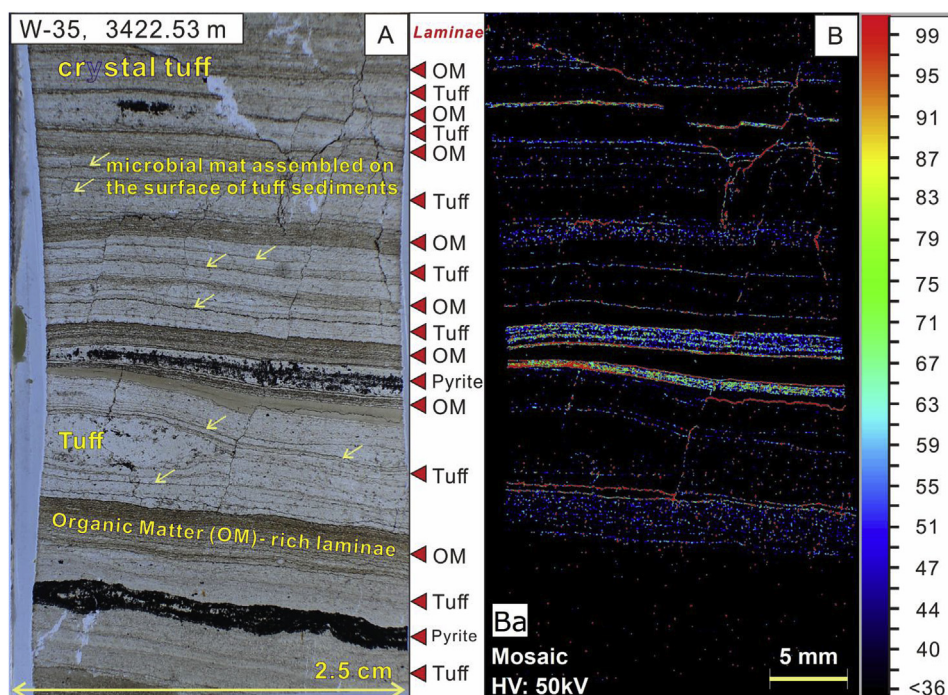


**Fig. 7.** Lithofacies composed of coupled dark-colored organic matter-rich laminae (OM) and light-colored organic-poor tuff laminae (Tuff) (well W-35, 3422.53 m). (A) Microbial mats assembled at the surfaces of tuff layers to formed organic-rich laminae, and are revealed in darker colors in the laminated interfaces. (B) The element of Ba indicates that organic-rich laminae have higher Ba content compared to the tuff laminae. (For interpretation of the references to color in this figure legend, the reader is referred to the Web version of this article.)

they occur in evaporite-rich, and clay-poor lacustrine strata, and major types of stylolite can be found in the Fengcheng Formation and have some special characteristics (Figs. 7, 13–15, 17). The characteristics of representative stylolite are as follows.

Based on the core section data, sedimentary stylolites and tectonic stylolites can be identified easily (Fig. 13). In some core sections, evaporites (dominated by shortite, reedmergnerite, and dolomite) have accumulated and occur as layers that alternate with evaporite-poor layers. Sedimentary stylolites occur at the contact interfaces between evaporite-rich layers and evaporite-poor layers, and they are parallel to the contact interfaces. Tectonic stylolites also occur in the core sections, and they formed by further pressure solution of previous fractures (Fig. 13A–B). Deformation structures commonly occur in evaporite-bearing source rocks, and organic matter accumulates in the stylolites

(Fig. 13I–J). All the stylolites have low amplitudes.

In the evaporite-poor samples, low-amplitude stylolites also occur along the contact interfaces between different lithological laminae (Fig. 7). Take the sample in well W-35 (3422.53 m) as an example. Few evaporite minerals occur here, and this thin section photograph shows that organic-rich laminae alternate with organic-poor tuff laminae. The sedimentary stylolites form in the contact interfaces between different lithological laminae, and most of them are filled by organic matter. This type of source rock formed in the shallow lake margin and was dominated by volcanic eruption-related sediments, with few evaporite minerals and carbonates.

Fine-grained dolomite-rich rocks are another type of representative high-quality source rocks, in which many stylolites occur (Fig. 14). Most of the stylolites are bed-parallel and have low amplitudes

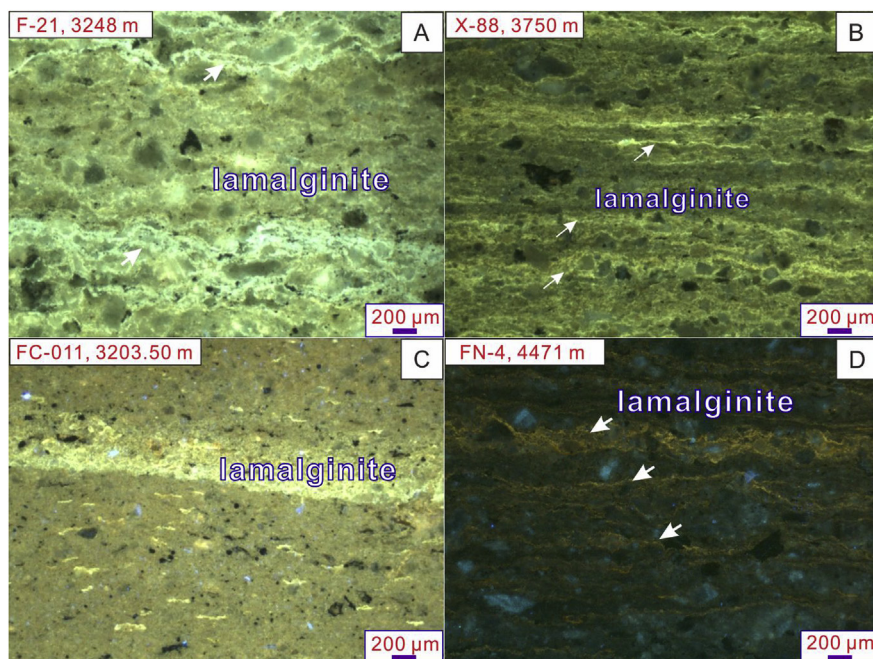


**Fig. 8.** Characteristics of organic-rich source rocks from shallow lake margins. (A) Wavy lamalginite laminae, the Fengcheng Formation, well F-21, 3248 m. Lamalginite laminae are continuous and abundant, which reflects algal bloom in warm seasons. (B) Wavy lamalginite laminae alternating with organic-poor felsic grain laminae, the Fengcheng Formation, well X-88, 3750 m. (C) Lamalginite assembled in the upper part of this view, while certain other organic matter fragments are scattered in the organic-poor matrix, the Fengcheng Formation, well FC-011, 3203.50 m. (D) Lamalginite occurring as continuous laminae and alternating with felsic grain sediment, the Fengcheng Formation, well FN-4, 4471 m.

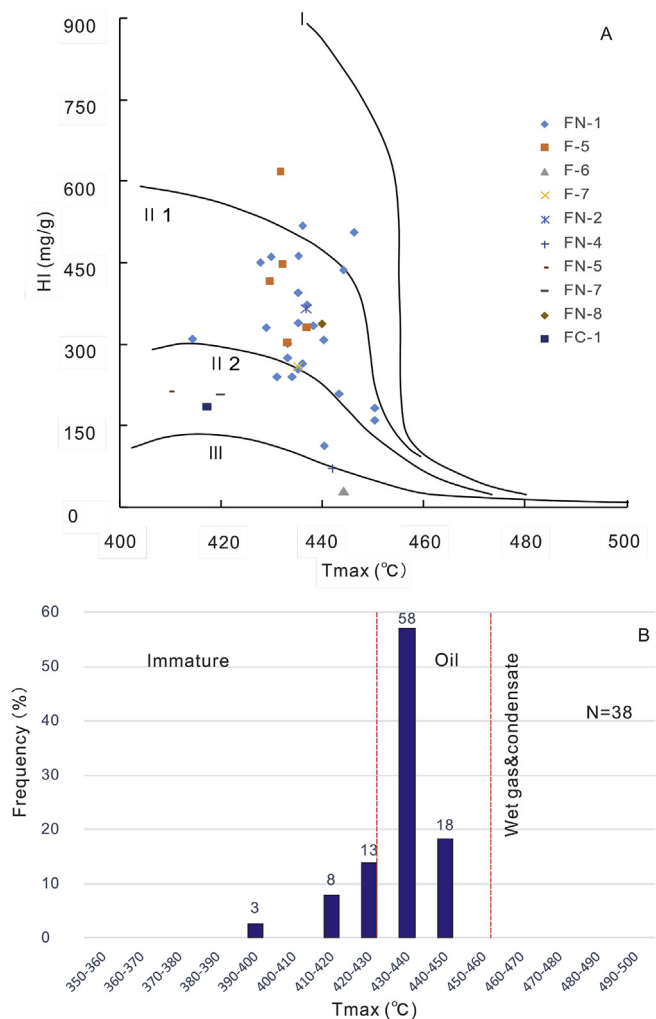


**Fig. 9.** Organic matter types and associated maturity in the Fengcheng Formation. (A) Kerogen-type differentiation plot of the source rocks in the Fengcheng Formation. Three outlier samples with abnormally high Ro values (> 3.0) were not used (FN-1, 4195.31 m; FN-1, 4233.17 m; FN-3, 3909.36 m). (B) The frequency of Tmax in the Fengcheng Formation.

(Fig. 14A–B). Faint yellow hydrocarbon residues are visible in the bed-parallel stylolites (Fig. 14C). The finely crystalline dolomitic rock has been cut into countless dolomitic lenses (Fig. 14C–E). The residues in stylolites are dominated by quartz and feldspars, and there are few clay minerals (Fig. 14E). The elements Mg, Si, and Ca in the micro-XRF image of whole thin section reflect the relationship between lentic dolomites and felsic background. The fine-crystalline dolomitic rocks were cut into countless isolated lenses or interrupted chains, and the felsic matrix connected in the whole thin sections (Fig. 15A). The contact interfaces between dolomitic lenses and felsic residues in stylolites are uneven, and there are dolomite residues left in the stylolites (Fig. 15B–C). Faint yellow hydrocarbons exist in the felsic residues in stylolites (Fig. 15D–E).

5.3. Expulsion fractures

Expulsion fractures are laminae-parallel and commonly developed in organic-rich shales; these fractures are caused by hydrocarbon generation from kerogens and can be distinguished to tectonic fractures by their occurrences: uneven fracture walls and deformation of laminae because of local overpressures, and not cutting through all laminae (Teixeira et al., 2017). Expulsion fractures are widely developed in the fine-grained organic-rich source rocks in the Fengcheng Formation. Kerogens are abundant in some samples and occur parallel to laminae (Fig. 16). Expulsion fractures commonly develop at the edges of the linear kerogens. The walls of the expulsion fractures are uneven and bypass particles (Fig. 16A–B). The mineral compositions of kerogen-rich source rocks as seen under the microscope reveal that few clays exist and that the composition is dominated by hard particles such as quartz, feldspar, and dolomites (Fig. 16A–B). As a result, when organic matter matured, expulsion fractures formed by splitting different hard particles, and they appear as wavy occurrences bypassing hard particles. Expulsion fractures generated from different kerogens become closer and closer and eventually connect to form expulsion fracture networks (Fig. 16A–C). Carbonates are common minerals occurring in this type of kerogen-rich source rock, and expulsion fractures and kerogens usually connect these carbonate assemblages (Fig. 16C–D). These carbonates are diagenetic minerals, which demonstrates that kerogens and expulsion fractures formed path networks. This kind of network provides favorable paths for the migration of diagenetic fluids, including liquid hydrocarbons.

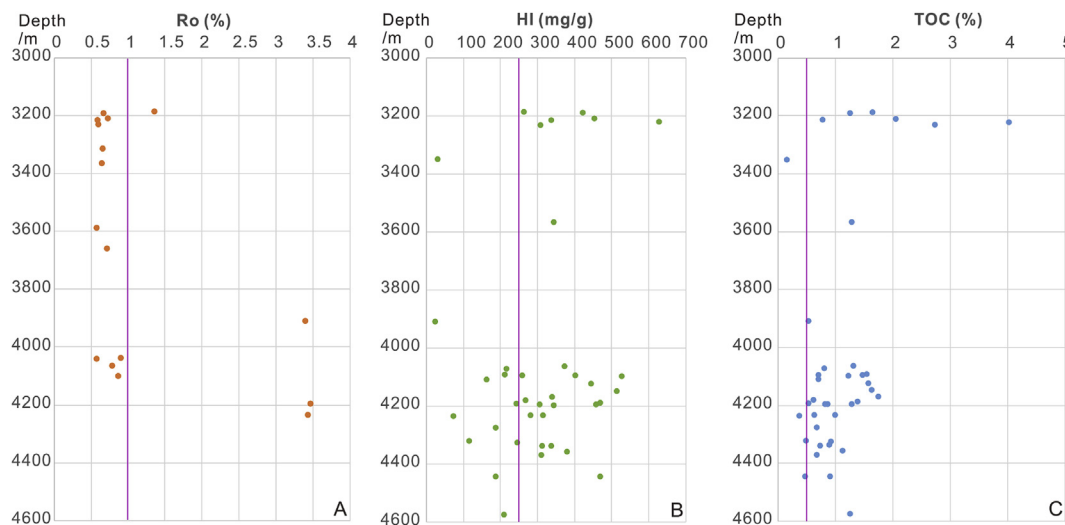


**Fig. 10.** The transformation of Ro, HI and TOC versus depth. (A) The vertical distribution of Ro. Most of the values are less than 1.0, which indicates that the kerogens are mature and in the oil window. There are three abnormal values larger than 3.0 may have been caused by thermal or magmatic events. (B) The vertical distribution of HI. Most of the values are higher than 250 mg/g, which indicates that the kerogens are mature and in the oil window. (C) the vertical distribution of TOC. Most of the values are higher than 0.5%, which indicates that the kerogens are mature and in the oil window.

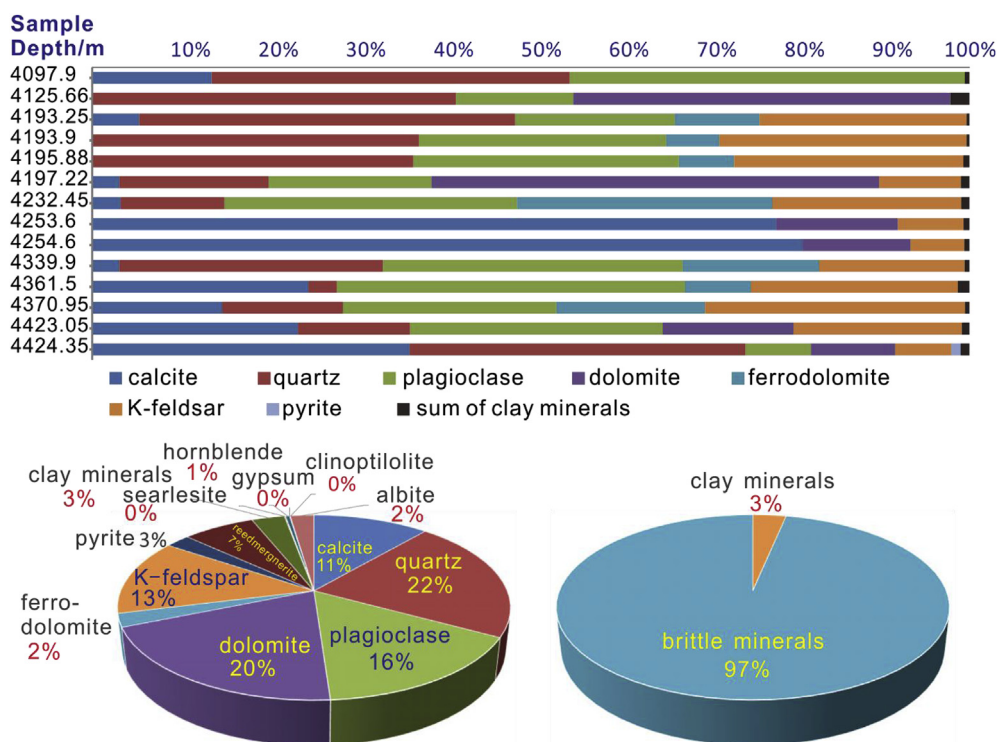


Fig. 11. The mineral composition of source rocks in well FN-1. The overall content of clay minerals is very low, whereas brittle minerals are common.

In Fig. 7, we characterize the organic-rich tuffs based on an overview of thin sections, and we determine that organic-rich laminae (microbial mats) alternated with organic-poor tuff laminae. Stylolites occur at the contact interfaces between different lithological laminae. Furthermore, representative hydrocarbon expulsion fractures developed in the organic-rich laminae (Fig. 17A–C). Dense expulsion fractures developed in organic-rich laminae, and hard particles rotated because of the expulsion of hydrocarbons (Fig. 17B), while laminae-parallel stylolites developed in crystal tuff laminae (Fig. 17C).

5.4. Fractures and microfractures

The term microfracture refers to fractures visible only under magnification, having lengths of millimeters or less and widths generally less than 0.1 mm (Anders et al., 2014). Fractures and microfractures caused by tectonic activity develop in all kinds of organic-rich source rocks associated with other paths for hydrocarbon expulsions and migrations. Fractures are the important paths that connect organic-rich laminae and organic-poor laminae (Fig. 7). They commonly have high angles, are filled by bitumen and cut through different laminae (Fig. 7). Some stylolites evolve from fractures by pressure solution and occur with low amplitudes (Fig. 13A–B), while other fractures have not yet evolved into stylolites and are unfilled (Fig. 13C–F). There are some microfractures filled by authigenic cherts (Fig. 14A–B). High-angle microfractures connect other paths (hydrocarbon expulsion fractures and stylolites) and form 3-D path networks (Fig. 17A).

6. Discussion

6.1. An alkaline saline lake is a favorable depositional environment for organic-rich source rocks and organic matter dominated by microbial mats

6.1.1. Paleoenvironmental conditions for source rocks

The alkaline saline lakes are favorable environments for high-quality organic-rich source rocks. e.g., the Eocene Green River Formation in the alkaline Piceance Creek Basin developed one of the

richest oil shale resources known, where kerogen-rich mudstones exist over most of the basin (Tănăvsuu-Milkevičienė and Sarg, 2012; Birdwell et al., 2013). The lithological characteristics of the source rocks are shown as alternating kerogen-rich laminae and kerogen-poor laminae in the Green River Formation in the nearby Fossil Basin (Buchheim, 1994). Previous study also demonstrated that bacteria and algae were dominant biological sources and contributing to source rocks in hydrological closed saline lakes (Warren, 2006, 2010; Luo et al., 2018a,b).

The lateral distribution of microbial mat-bearing source rocks and associated lithofacies was strongly influenced by the sediment amounts that were deposited at the margins of the lake. The continuous deposition of organic matter and felsic particles indicated there were few sediments transported into the depocenter during arid climates and high-salinity brine was suitable for microbial mats blooming, while discontinuous kerogens reflect the dominance of inflow processes in the deposition during humid climates. Wells AK-1 and FN-7 are the wells nearest to the basin center to date, and the lithofacies in these two wells represent deposition in the depocenter (Figs. 3–5). Because of long distances to the shore, lake-generated organics (microbial mats) were the least diluted by sedimentation. As a result, they could be preserved very well, and most of them showed as continuous dark colored organic-rich laminae (Figs. 4 and 5).

Wells FN-1, FN-4, W-35, X-88, FC-011, and F-21 are not located in the basin center and are much closer to the shore. The content of organics decreased, and some organics, including hydrothermal-related microbial mats and algae occurred in the shallow lake margins.

6.1.2. Benthic microbial mats are the dominant organics

Organic-rich oil shale can form in some extremely arid depositional environments such as deserts, and oil shale can originate from algal ooze that forms in the bottom of shallow, spring-fed lakes (Bradley, 1973). Modern microbial mats commonly occur in shallow lake margins where hot springs are flowing out, e.g., Champagne pool in Waitotapu, New Zealand (Handley et al., 2005); Pavlova spring in Ngatamariki, New Zealand (Campbell et al., 2002); the silica hydrothermal system at

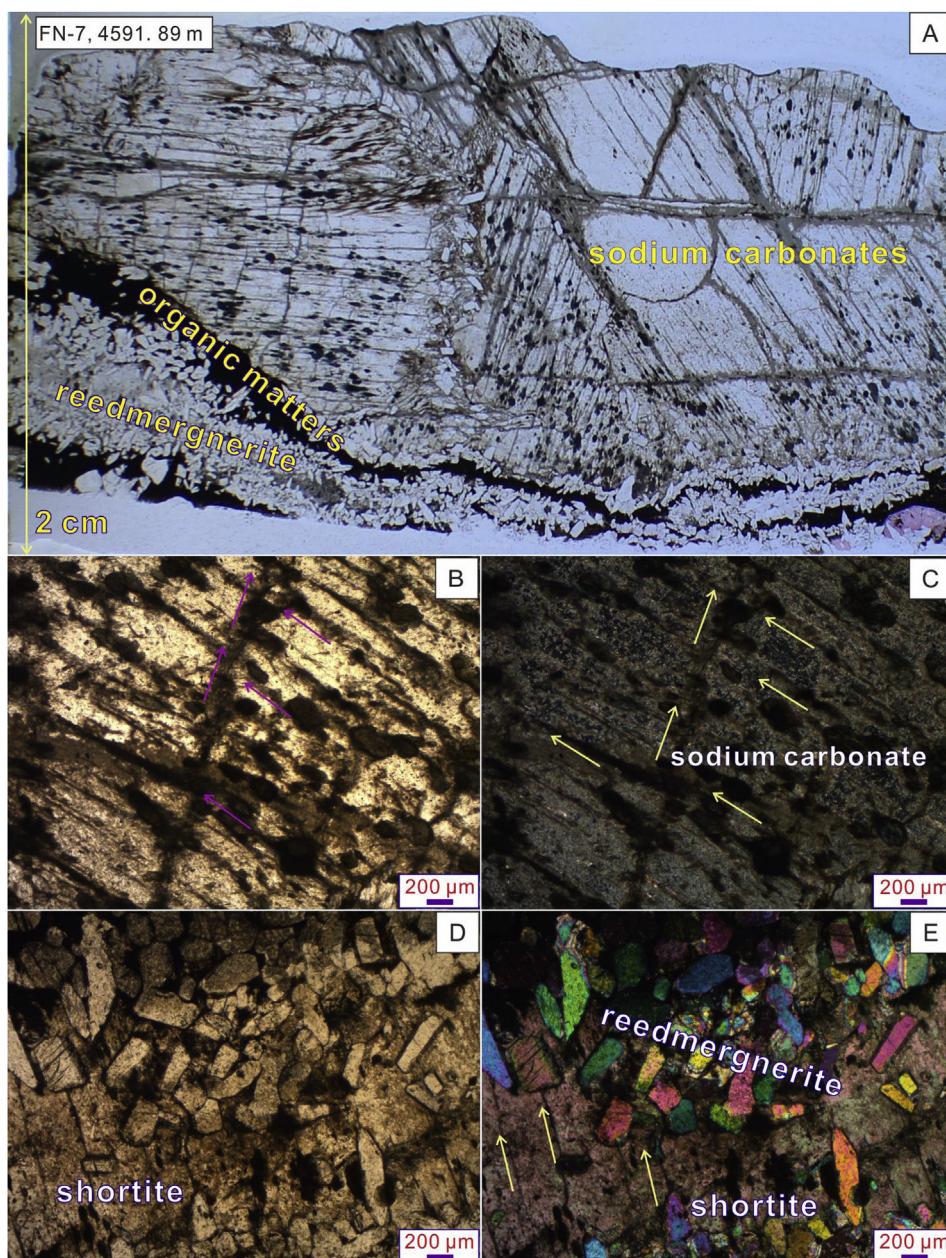


**Fig. 12.** Characteristics of organic matters in the bedded sodium carbonates layer. (A) Characteristics of organic matters in the thin section, which occurred in the contact interface between large-sized sodium carbonates and other evaporites, and intergranular seams. Well FN-7, 4591.89 m, (B) Zooming characteristics of intergranular seams under microscope, plane-polarized light, well FN-7, 4591.89 m, (C) Zooming characteristics of intergranular seams under microscope, cross-polarized light, well FN-7, 4591.89 m, (D) Characteristics of shortite and reedmergnerite under microscope, plane-polarized light, well FN-7, 4591.89 m, (E) Characteristics of shortite and reedmergnerite under microscope, cross-polarized light, well FN-7, 4591.89 m.

Lake Baringo in the Kenya Rift Valley (Buatois et al., 2017); the outflow channel of Queen's Laundry hot spring (Siljeström et al., 2017), the Hundred Spring Plain of the Norris Basin (Lalonde et al., 2007), and Stinking Springs in northwestern Utah, USA (Bonny and Jones, 2007); Arctic hot spring in Greenland (Roeselers et al., 2007); hot springs in Araro, Mexico (Prieto-Barajas et al., 2017); the hydrothermal system at Mangatete, Taupo Volcanic Zone, New Zealand (Drake et al., 2014); hot springs in Yellowstone National Park (Jahnke et al., 2004; Zhang et al., 2004; King et al., 2006; Berelson et al., 2011; Fouke, 2011; Osburn et al., 2011); the hot spring in Yunnan, China (Jones and Peng, 2016); Loburu hot springs in Lake Bogoria, Kenya Rift Valley (Renaut et al., 1998); and the hot springs in northern Chile (Fernandez-Turiel et al., 2005). The microbial mats accumulate under the brines or around the hot springs as alternating microbial mat-rich and microbial mat-poor laminae.

When the Fengcheng Formation was deposited, hot springs must have been the important controlling factor along with frequent volcanic activities, which offered favorable environments for microorganism growth. The well-preserved microbial mats presented in Fig. 6 probably

indicate the wide existence of microbial deposition in the study area. Previous study has demonstrated that when the lower part of the Fengcheng Formation was deposited, a volcanic cluster in well-block FN-1 occurred and that associated hot springs must have provided favorable environments for microbial mats to accumulate. The microbial mats are easily destroyed and need strict preservation conditions (Schieber, 1999); thus, both the widely distributed continuous and the discontinuous microbial mats in the Fengcheng Formation may demonstrate that there were many more microbial mats than the amount preserved in the strata. The microbial mats in Fig. 6 have not been destroyed along with burial, and the other sediments consist of sand-sized particles. These characteristics demonstrate that they formed in the shallow lake margin and were perpetually covered by water. If they had formed in the periodically exposed shoreline, the reworking of sediments would have been intense, and the microbial mats could not have been preserved well. If they had formed in the oxygen-deprived depocenter, the felsic particles must have been very fine grained. In addition, the color is not so dark, and therefore, these microbial mats must have formed in the low-angle, low-energy, shallow and perennial

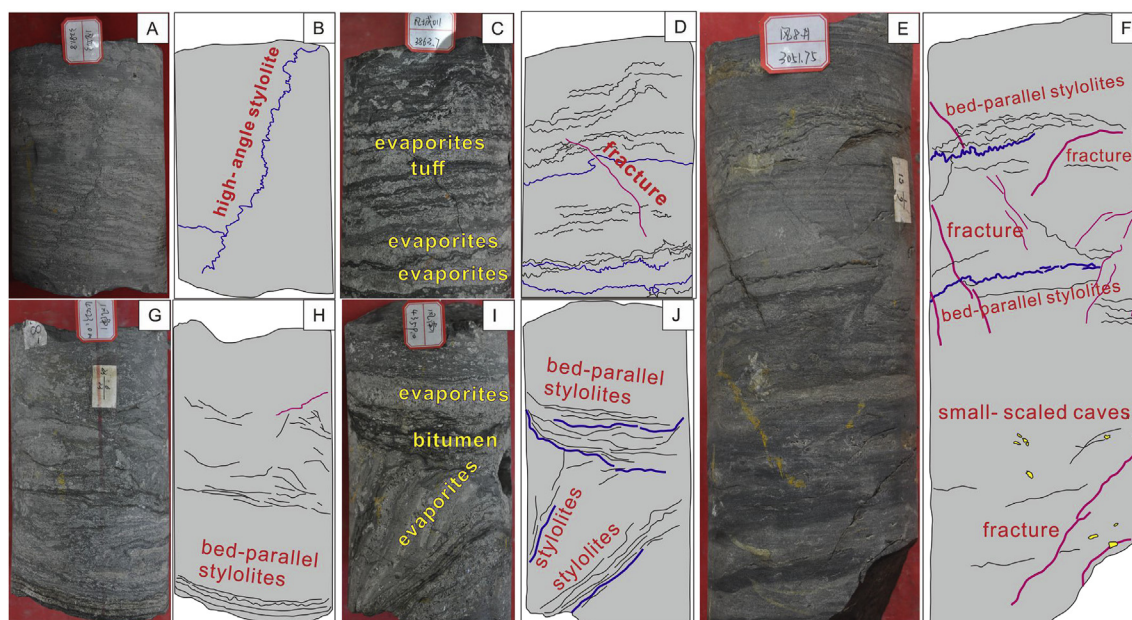


**Fig. 13.** Characteristics of stylolites from the core sections. Sedimentary stylolite occurred at the contact interface between evaporites-rich layer and evaporites-poor layer, and it paralleled to the contact interface. Tectonic stylolite also occurred in core sections, which formed by further pressure solutions of previous fractures.

lake margin.

The characteristics of the microbial mats in both the shallow lake margins and the deep lake center show that the organic matters are dominated by benthic microbial mats. In the northeastern part of the study area, intense volcanic eruptions occurred, and volcanic sediments dominate. Microbial mat-rich laminae alternate with tuff/tuffaceous sediments-rich laminae, which demonstrates that microbial mats accumulated at the bottom of nutrient-rich shallow water as laminae in the intervals between volcanic eruptions (Fig. 7). Microbial mats have also played an important role in deep-water oxygen-deprived settings, which form high-quality evaporite-bearing source rocks (Fig. 5). Microbial mats can live under extreme conditions, and they colonized, stabilized, and modified the surfaces of other fine-grained sediments. In this study, they occurred on the surfaces of fine-grained sediments laminae (Figs. 4, 5 and 7). The arid depositional environments caused low sedimentation rates, and volcanic eruptions produced abundant nutrients along with fine-grained ashes and dusts. Additionally, hot springs may have occurred around volcano clusters. The environments may have been suitable for microbial communities to thrive and be preserved.

In addition to the benthic microbial mats that occurred in the shallow lake margins and the deep lake center, lamalginites also bloomed at the surface of the brines. The volcanic eruptions provided plentiful nutrients, which provided suitable environments for algae.

### 6.1.3. Hydrocarbon potentials of the source rocks

When the Fengcheng Formation deposited, the ancient Mahu Lake was a rare alkaline lake with a closed hydrological system (Yu et al., 2016a,b). The lithological correlations across wells AK-1, FN-7, FN-1, and FN-4 show that organic matter can occur and be preserved in most depositional subenvironments: lake margins near the shore, shallow lake margins, and the slope to the lake depocenter (Fig. 3). In particular, the lithologic columns that represent the depocenter (wells AK-1 and FN-1) have great thicknesses of fine-grained sedimentary rocks. The source kitchens in the Fengcheng Formation are located at the center of the Mahu Sag (Liu et al., 2013). Representative organic-rich rocks in lower and middle parts of the Fengcheng Formation demonstrate that the source rocks in depocenters have high total organic contents. Previous studies and data from this study suggest that source rocks in the Fengcheng Formation are dominated by type II kerogen and

have entered into the low mature-mature evolution stage (Hu et al., 2016, 2017; Ren et al., 2017). Each of the hydrocarbon source rock evaluation indices; kerogen types, Tmax, Ro, HI, and TOC demonstrate that the source rocks of the Fengcheng Formation are high-quality and have prolific hydrocarbon generation potential (Figs. 9 and 10). Based on data from various references and Xingjiang Oilfield Company we conclude that the kerogens in the Fengcheng Formation are dominated by Type II<sub>1</sub> and are beneficial to generate oil (Tissot and Welte, 1984b); this excludes the anomalous samples with Ro higher than 3.0 which, again, do not accurately represent the source rocks of the Fengcheng Formation as they may have been affected by abnormal hydrothermal events. Again, the indices Ro, Tmax, HI and TOC all show that most of the hydrocarbon source rocks have entered into the oil generation window and have hydrocarbon generation potential.

Additionally, the high-quality source rocks in the Fengcheng Formation have large volumes. Some studies show that the extent of the Fengcheng Formation is much greater than we know, even extending to the area beyond the Halalate Mountains, and 1000 km<sup>2</sup> more high-quality source rocks have been found compared to the previous recognition about the extent of source rocks in the Fengcheng Formation (Wang et al., 2014). Compared to the indices of other strata in the Permian Mahu Sag, the source rock indices in the Fengcheng Formation show high organic matter abundance, good type and strong hydrocarbon generation capacity (Cao et al., 2015). Plentiful algae and microbes result in continuous hydrocarbon generation with high-quality oil and gas (Cao et al., 2015; Ren et al., 2017).

## 6.2. Multiple paths join to enhance the efficiencies of hydrocarbon expulsion and migration

### 6.2.1. Lithofacies associations promote hydrocarbon expulsion and migration

The lithofacies associations in most saline lakes occur as alternating evaporite layers and organic-rich oil shale layers (Zhang et al., 2005). The layer located between two evaporite layers is a very prominent assemblage of hydrocarbon reservoir and source rocks (Fang, 2002). In some cases, the richest oil shale is composed of a mixture of alkaline earth carbonates and organic constituents (Surdam and Wolfbauer, 1973; Desborough, 1978; Birdwell, 2012; Jagniecki and Lowenstein, 2015). In some moderate saline lakes, organic-rich oil shales may

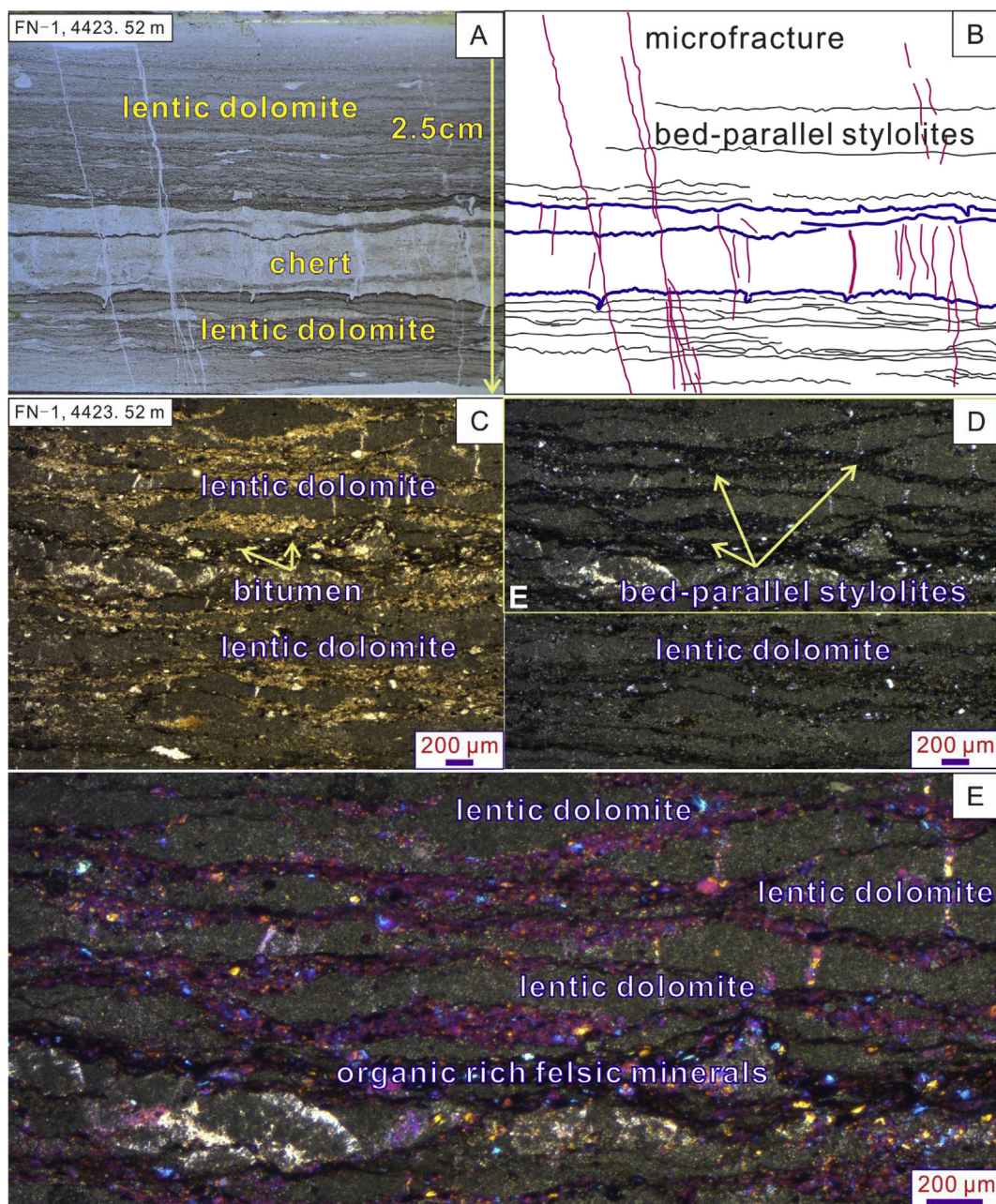


**Fig. 14.** Characteristics of low-amplitude Bed-parallel stylolites in the dolomitic tuff. (A) Most of the stylolites paralleled to the laminae interfaces from the thin section, well FN-1, 4423.52 m, (B) Sketch map of the (A), most of the stylolites paralleled to the laminae interfaces, and commonly cut through by microfractures, well FN-1, 4423.52 m, (C) Rocks are cut into dolomitic lenses by stylolites, plane-polarized light, well FN-1, 4423.52 m, (D) Rocks are cut into dolomitic lenses by stylolites, cross-polarized light, well FN-1, 4423.52 m, (E) Zooming characteristics of stylolites and dolomitic lenses. Stylolites residues are dominated by felsic minerals, with few clay minerals, cross-polarized light and adding gypsum test plate, well FN-1, 4423.52 m.

alternate with calcite or dolomite laminae (Liang et al., 2017, 2018).

In this study, the dark-colored organic-rich sediments occur associated with evaporites in most subenvironments, especially in the depocenter and the transitional zone between the depocenter and the lake margins near the shore. The representative lithofacies of the lower Fengcheng Formation show that the evaporite laminae alternate with organic-rich laminae frequently, and a single lamina is very thin; most of them are only a few millimeters thick (Fig. 4). The representative lithofacies of the middle Fengcheng Formation show that bedded sodium carbonates alternate with organic-rich fine-grained rocks (Fig. 5B–E), and the dark-colored layers show as well-preserved benthic microbial mats, while the light-colored sodium carbonates layers developed intergranular seams (Fig. 12). The representative lithofacies

formed in the transitional zone or shallow lake margins showed alternating microbial mat-rich laminae and microbial mat-poor laminae (Figs. 6, 7 and 13). The lithofacies associations above are beneficial to hydrocarbon expulsion and migration.

- ① Evaporite laminae or layers provided paths for the hydrocarbon expulsions and migrations. If the fine-grained organic-rich source rocks were massive, the hydrocarbons could not be easily discharged from the low-permeability source rocks. The intergranular seams played an important role in providing paths for hydrocarbons expelled out of adjacent organic-rich source rocks (Fig. 12). Repeated evaporite layer/lamina and organic-rich source rock layer/lamina couplets promoted hydrocarbon expulsion efficiency.

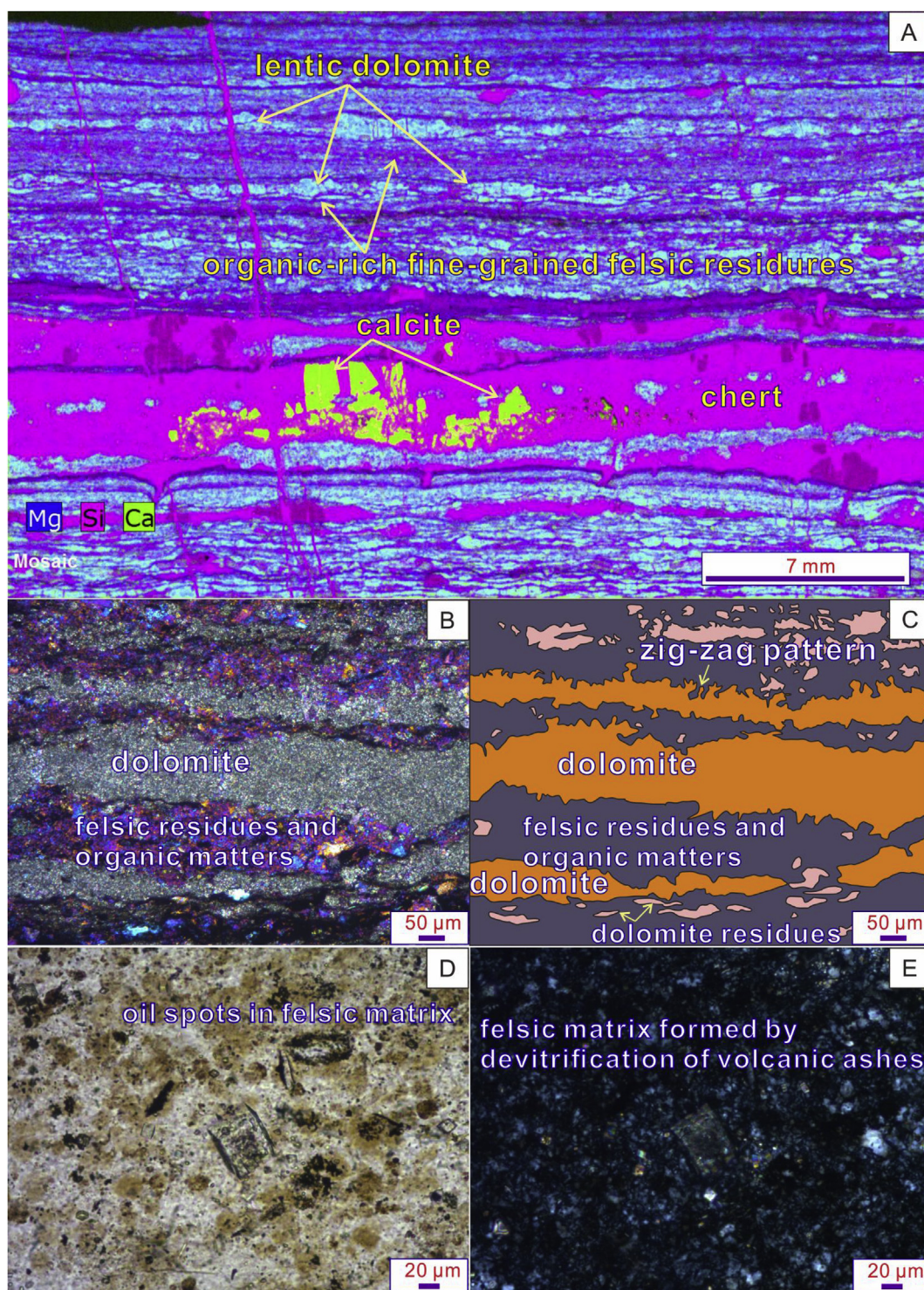


**Fig. 15.** Characteristics of low-amplitude bed-parallel stylolites in the dolomitic tuff (the same sample as Fig. 14). (A) The major elements Mg, Si, and Ca in the micro-XRF image. The combinations of the elements Mg and Ca indicate the distribution of dolomites. The generalized occurrences of lentic dolomites and felsic matrix. The scanning extent is the same as the thin section in Fig. 14A. (B) The characteristics of the contact interface between the dolomite laminae and the stylolite residues. Cross-polarized light with gypsum test plate inserted, well FN-1, 4423.52 m. (C) Sketch map of the (B). The contact interface between dolomite laminae and stylolites occurred as a zig-zag pattern, well FN-1, 4423.52 m. (D) Hydrocarbon accumulation in the stylolites, plane-polarized light, well FN-1, 4423.52 m. (E) Hydrocarbon accumulation in the stylolites, cross-polarized light, well FN-1, 4423.52 m.

© The interaction of source rocks and oil with evaporites in saline lake facies may enhance the efficiency of hydrocarbon generation. Indeed, “organic-inorganic interactions in petroleum-producing sedimentary basins” has recently become a popular topic. Inorganic compounds such as water and minerals participate as reactants or

catalysts during organic matter maturation (Seewald, 2003; Schulz et al., 2016), especially in the areas of clastic diagenesis (Edman and Surdam, 1986; MacGowan and Surdam, 1990) and carbonate diagenesis (Schulz et al., 2017). Thus far, previous studies dealing with the general topic “inorganic mineral” influences on kerogen

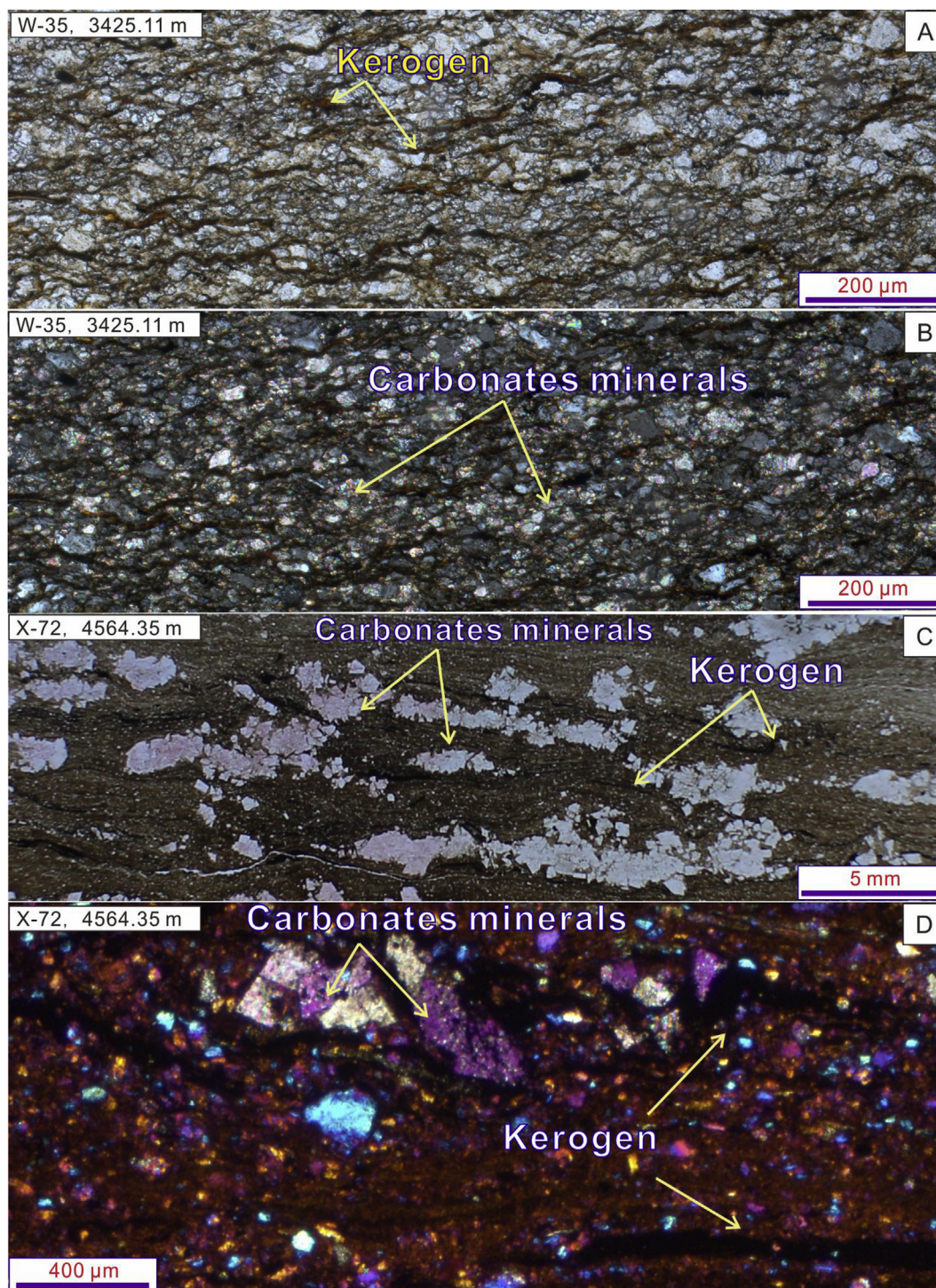
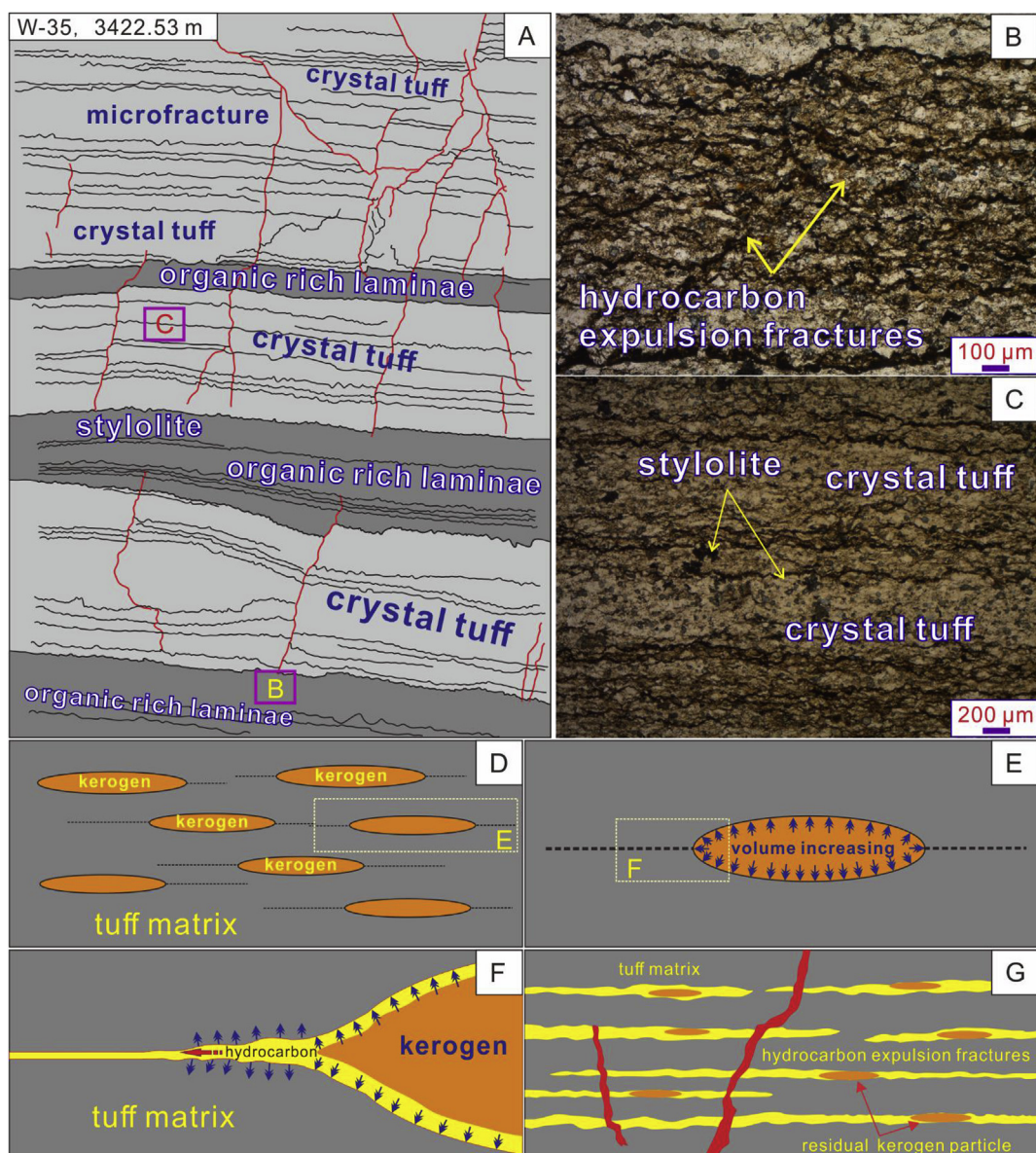


Fig. 16. Hydrocarbon expulsion fractures in the source rocks in the Fengcheng Formation. (A) The kerogens paralleled in the dolomitic tuff, plane-polarized light, well W-35, 3425.11 m. (B) The kerogens paralleled in the dolomitic tuff, cross-polarized light, well W-35, 3425.11 m. (C) The distribution of kerogens and relationships between laminated tuff, carbonates assemblages and kerogen, photograph of thin section, well X-72, 4564.35 m. (D) The distribution of kerogens and relationships between laminated tuff, carbonates assemblages and kerogen under microscope, cross-polarized light adding gypsum test plate, well X-72, 4564.35 m.

pyrolysis and oil hydrocarbon generation” have been predominantly focused on the following areas: ① the effects of clay catalysis on hydrocarbon generation (Pan et al., 2010; Rahman et al., 2017, 2018; Bu et al., 2017); ② the catalytic effect of nickel and magnetite during coal pyrolysis (Gao et al., 2018); ③ the catalytic effect of iron-bearing minerals on hydrocarbon generation (Ma et al., 2016a,b; Ma et al., 2018); and ④ the catalytic effect of calcite on hydrocarbon generation (Pan et al., 2010). There is few paper in English that have

discussed the catalytic effects of evaporites, carbonates, halite, and gypsum that formed in evaporite lakes on hydrocarbon generation. Rather, the majority of studies dealing with this topic are instead published in Chinese. These experiment-based Chinese studies have demonstrated that evaporites play an important role in the catalysis of oil and gas generation (Wang, 2009; Jin et al., 2010). Moreover, these studies have shown that carbonates, gypsum, and sodium chlorite catalyzed intensely on organic matter; e.g., by adding



**Fig. 17.** Combination of multiple paths enhancing the hydrocarbon expulsion and migration efficiencies. (A) Sketch map of Fig. 7. Organic-rich laminae alternated with organic-poor tuff laminae, and the combination of hydrocarbon expulsion fractures, stylolites, and microfractures formed network for hydrocarbon migration. Well W-35, 3422.53 m. (B) Hydrocarbon expulsion fractures occurred in the organic-rich laminae, plane-polarized light, well W-35, 3422.53 m. (C) Stylolites occurred in the organic-poor tuff laminae, plane-polarized light, well W-35, 3422.53 m. (D–E) The model of the development patterns of hydrocarbon expulsion fractures.

carbonate or gypsum to the source rock material, the number of catalyzing hydrocarbons would rise 34% and 28%, respectively (Wang, 2009). In the Fengcheng Formation, the evaporites have various occurrences, e.g., bedded evaporites alternating with kerogen-rich source rocks (Figs. 4 and 5), evaporite mineral nodules scattered in the source rocks (Fig. 5), and diagenetic evaporites occurring in the source rocks (Figs. 4 and 5). The evaporites may indeed have catalyzed the hydrocarbon generation and pyrolysis. Despite the paucity of studies on the catalytic effect of evaporite minerals on hydrocarbon generation, it is generally acknowledged that source rocks that occurred with evaporites are commonly of high-quality. Certainly, the interactions between evaporite minerals and kerogen/hydrocarbon should be further studied.

- ③ The contact interfaces between evaporite layers/laminae and organic-rich source rocks are easily dissolved and form favorable pathways for oil and gas migration. The stylolites are easily generated from the contact interfaces in evaporite-bearing strata, and

they are commonly filled by bitumen, which shows that they were favorable pathways for hydrocarbon expulsion and migration (Bauerle et al., 2000). The contact interface between the bedded sodium carbonates and source rocks is also filled by organic matter (Fig. 12), and the contact interfaces between evaporite laminae and dark-colored source rocks are also favorable positions for stylolite formation (Fig. 12). The alternations of evaporite lithofacies and non-evaporites lithofacies are good for hydrocarbon expulsion in time.

#### 6.2.2. High content of brittle minerals is the basis for low-amplitude stylolites

The stylolites can be classified and described according to their amplitudes (Koehn et al., 2007, 2016), and the amplitudes can be used to calculate the rock loss formed by pressure dissolution (Ramos, 2001; Ben-Itzhak et al., 2012). Most of the stylolites in the Fengcheng Formation have low amplitudes (Figs. 13–15, 17), which is very different

from those stylolites occurring in the carbonate strata. The mineral compositions of rocks in the Fengcheng Formation show high brittle minerals contents, and the sum of the clay minerals is very low. Additionally, the carbonate minerals are scattered within the source rocks, and there are few rocks that consist entirely of carbonates (calcites or dolomites). As a result, the rock loss formed by dissolution along laminated interfaces or microfractures under compressive stress conditions is not as great as that in carbonate strata. Taking the sample in Fig. 14 as an example, the primary rocks may consist of relatively homogeneous finely crystalline dolomitic rocks. Dolomites dissolve along laminated interfaces and the insoluble mineral residues are dominated by felsic minerals, in which few clay minerals are included (Figs. 14 and 15). The contact interfaces between finely crystalline laminae and residues in the stylolite show as zig-zag patterns (Fig. 15B–C), and hydrocarbon appear in the stylolites (Fig. 15D–E). In summary, the high content of brittle minerals, low content of clay minerals, and uneven distribution of dissolving minerals (calcite, dolomite) control the formation of low-amplitude stylolites. The low content of clay minerals in the residues in stylolites makes them favorable paths for hydrocarbon expulsion and migration.

### 6.2.3. Combination of multiple paths promoted the efficiency of hydrocarbon expulsion and migration

The types of hydrocarbon expulsion and migration paths not only are various but also combine to form path networks. Taking the sample in Fig. 17 as an example, the paths consist of hydrocarbon expulsion fractures, stylolites, and microfractures. They are connected very well, and hydrocarbons can be expelled and migrate easily. The hydrocarbon expulsion and migration processes can be described as follows.

- ① The hydrocarbon expulsion fractures formed along with kerogen maturation. The organic matter was dominated by microbial mats and laterally extended along laminated interfaces. When the kerogens matured, the kerogen volumes increased, and microfractures along the laminated interfaces formed. As a result, kerogens and expulsion fractures connected to form networks in the organic-rich laminae. The model of the development patterns of hydrocarbon expulsion fractures is same as those that occur in typical oil shales (Fig. 17D–G) (Ougier-Simonin et al., 2016; Ma et al., 2017; Teixeira et al., 2017).
- ② The hydrocarbons migrated along stylolites. Most of the stylolites in the Fengcheng Formation have low amplitude and low amounts of clay minerals in the dissolution residues, which produces favorable paths for hydrocarbon migration rather than barriers. Even in carbonate strata, the stylolites are not continuous high-density layers and do not impact regional fluid flow (Heap et al., 2014; Baud et al., 2014). In most cases, the stylolites served as paths of migration for oil (Mileshina and Moskalev, 1962; Zhong et al., 2010; Martín-Martín et al., 2017). The low amplitudes of stylolites and the low clay minerals in stylolite dissolution residues in the Fengcheng Formation suggest that these stylolites are much superior to those in carbonate strata for hydrocarbon migration.
- ③ Fractures and microfractures provided paths for hydrocarbons to migrate for long distances. These fractures formed by tectonic activity and usually cut through laminated source rocks. Organic-rich laminae alternated with organic-poor tuff laminae in this sample (Fig. 17A). If there were no fractures or microfractures, the hydrocarbon could not migrate easily for a long time. When the fractures and microfractures cut through the laminated source rock, the hydrocarbons that migrated from organic-rich laminae along expulsion fractures and stylolites accumulated in the fractures and microfractures and migrated to the oil pool.

## 7. Conclusions

- 1) The Fengcheng Formation developed large volumes of high-quality

source rocks in an alkaline saline lake. The organic matter mainly formed in the basin and was not imported by runoff. Microbial mats were the dominant organic matter that could be formed in both the deep depocenter and the shallow lake area. Benthic microbial mats were preserved very well and generated hydrocarbons for overlying reservoirs. Algae bloomed at the shallow lake margins and provided the other important type of organic matter in the Fengcheng Formation. The source rocks in the Fengcheng Formation are dominated by type II<sub>1</sub> kerogen and have entered the low mature-mature evolution stage. Abundant algae and microbes resulted in continuous hydrocarbon generation.

- 2) Hydrocarbon expulsion fractures, stylolites, fractures and microfractures combined to form networks and enhanced the efficiencies of hydrocarbon expulsion and migration. Evaporite minerals may catalyze oil and gas generation in this lacustrine alkaline saline basin. At the same time, intergranular seams were important paths for oil and gas migration. Because of the high content of brittle minerals and the low clay contents, the stylolites were characterized by low amplitudes and high permeability. As a result, the stylolites provided favorable paths for hydrocarbon expulsion and migration. Combining hydrocarbon expulsion fractures in the organic-rich laminae and fractures and microfractures caused by compressive tectonic stress, networks formed, which enhanced the efficiencies of hydrocarbon expulsion and migration.

## Acknowledgements

This project was supported by the National Basic Research Program of China (973) (grant no. 2014CB239002), the Fundamental Research Funds for the Central Universities (grant no. 18CX02063A), the Fundamental Research Funds for the Central Universities (grant no. 16CX02030A) and the Natural Science Foundation of Shandong Province, China (grant no. ZR2014DQ016). The China University of Petroleum (East China) provided facilities for this research. We are grateful to the reviewers and the editor for the helpful comments to improve our paper.

## References

- Abouelresh, M.O., Slatt, R.M., 2012. Lithofacies and sequence stratigraphy of the barnett shale in east-central fort worth basin, Texas. AAPG (Am. Assoc. Pet. Geol.) Bull. 96, 1–22.
- Anders, M.H., Laubach, S.E., Scholz, C.H., 2014. Microfractures: a review. J. Struct. Geol. 69, 377–394.
- Baud, P., Heap, M.J., Reuschlé, T., Meredith, P.G., 2014. The impact of stylolites on fluid flow and rheology of porous carbonates. In: Eage Conference and Exhibition.
- Bauerle, G., Bornemann, O., Mauthe, F., Michalzik, D., 2000. Origin of stylolites in upper permian zechstein anhydrite (gorleben salt dome, Germany). J. Sediment. Res. 70, 726–737.
- Ben-Itzhak, L.L., Aharonov, E., Karcz, Z., Kaduri, M., Toussaint, R., 2014. Sedimentary stylolite networks and connectivity in limestone: large-scale field observations and implications for structure evolution. J. Struct. Geol. 63, 106–123.
- Ben-Itzhak, L.L., Aharonov, E., Toussaint, R., Sagy, A., 2012. Upper bound on stylolite roughness as indicator for amount of dissolution. Earth Planet Sci. Lett. 337–338, 186–196.
- Berelson, W.M., Corsetti, F.A., Pepe-Ranney, C., Hammond, D.E., Beaumont, W., Spear, J.R., 2011. Hot spring siliceous stromatolites from Yellowstone National Park: assessing growth rate and laminae formation. Geobiology 9, 411–424.
- Bian, W., Hornung, J., Liu, Z., Wang, P., Hinderer, M., 2010. Sedimentary and palaeoenvironmental evolution of the Junggar Basin, Xinjiang, northwest China. Palaeobiodivers. Palaeoenvir. 90, 175–186.
- Birdwell, J.E., 2012. Review of Rare Earth Element Concentrations in Oil Shales of the Eocene Green River Formation. U.S. Geological Survey Open-File Report 2012-1016, 20p.
- Birdwell, J.E., Johnson, R.C., Mercier, T.J., 2017. Organic Matter Distributions in Oil Shales Zones of the Green River Formation. Piceance Basin: paper NO. 135-6. Geological Society of America Annual Meeting, Seattle, WA.
- Birdwell, J.E., Mercier, T.J., Johnson, R.C., Brownfield, M.E., 2013. In-place Oil Shale Resources Examined by Grade in the Major Basins of the Green River Formation, Colorado, Utah, and Wyoming. U.S. Geological Survey Fact Sheet 2012-3145, 4p.
- Bonny, S.M., Jones, B., 2007. Diatom-mediated barite precipitation in microbial mats calcifying at Stinking Springs, a warm sulphur spring system in Northwestern Utah, USA. Sediment. Geol. 194, 223–244.
- Bradley, W.H., 1973. Oil shale formed in desert environment: green River Formation,

- Wyoming. *Geol. Soc. Am. Bull.* 84, 1121–1124.
- Bu, H., Yuan, P., Liu, H., Liu, D., Liu, J., He, H., Zhou, J., Song, H., Li, Z., 2017. Effects of complexation between organic matter (OM) and clay mineral on OM pyrolysis. *Geochem. Cosmochim. Acta* 212, 1–15.
- Buatois, L.A., Renaut, R.W., Scott, J.J., Owen, R.B., 2017. An unusual occurrence of the trace fossil *Vagorichnus* preserved in hydrothermal silica at Lake Baringo, Kenya Rift Valley: taphonomic and paleoenvironmental significance. *Palaeogeogr. Palaeoclimatol. Palaeoecol.* 485, 843–853.
- Buchheim, H.P., 1994. Paleoenvironments, lithofacies and varves of the fossil butte member of the Eocene Green River formation, southwestern Wyoming. *Contrib. Geol. Univ. Wyo.* 30, 3–14.
- Campbell, K.A., Rodgers, K.A., Brotheridge, J.M.A., Browne, P.R.L., 2002. An unusual modern silica-carbonate sinter from Pavlova spring, Ngatamariki, New Zealand. *Sedimentology* 49, 835–854.
- Cao, J., Lei, D., Li, Y., Tang, Y., Abulimit, Chang, Q., Wang, T., 2015. Ancient high-quality alkaline lacustrine source rocks discovered in the lower permian Fengcheng Formation, Junggar Basin (in Chinese). *Acta Pet. Sin.* 36, 781–790.
- Cao, J., Yao, S., Jin, Z., Hu, W., Zhang, Y., Wang, X., Zhang, Y., Tang, Y., 2006. Petroleum migration and mixing in the northwestern Junggar Basin (NW China): constraints from oil-bearing fluid inclusion analyses. *Org. Geochem.* 37, 827–846.
- Cao, J., Zhang, Y., Hu, W., Yao, S., Wang, X., Zhang, Y., Tang, Y., 2005. The Permian hybrid petroleum system in the northwest margin of the Junggar Basin, northwest China. *Mar. Petrol. Geol.* 22, 331–349.
- Chen, K.Y., Hu-Jun, H.E., Liu, B.J., Shi, Z.S., Shi, J., 2002. Geochemistry character in paleo-saline depositional system on Qianjiang group in Qianjiang depression. *J. Salt Lake Res.* 10, 19–24.
- Chen, Z., Wang, X., Zha, M., Zhang, Y., Cao, Y., Yang, D., Wu, K., Chen, Y., Yuan, G., 2016a. Characteristics and formation mechanisms of large volcanic rock oil reservoirs: a case study of the Carboniferous rocks in the Kebai fault zone of Junggar Basin, China. *AAPG (Am. Assoc. Pet. Geol.) Bull.* 100, 1585–1617.
- Chen, Z., Zha, M., Liu, K., Zhang, Y., Yang, D., Tang, Y., Wu, K., Chen, Y., 2016b. Origin and accumulation mechanisms of petroleum in the carboniferous volcanic rocks of the Kebai fault zone, western Junggar Basin, China. *J. Asian Earth Sci.* 127, 170–196.
- Desborough, G.A., 1978. A biogenic-chemical stratified lake model for the origin of oil shale of the Green River Formation: an alternative to the playa-lake model. *Geol. Soc. Am. Bull.* 89, 961.
- Drake, B.D., Campbell, K.A., Rowland, J.V., Guido, D.M., Browne, P.R.L., Rae, A., 2014. Evolution of a dynamic paleo-hydrothermal system at Mangatete, Taupo volcanic zone, New Zealand. *J. Volcanol. Geoth. Res.* 282, 19–35.
- Ebner, M., Koehn, D., Toussaint, R., Renard, F., Schmittbuhl, J., 2009. Stress sensitivity of stylolite morphology. *Earth Planet Sci. Lett.* 277, 394–398.
- Edman, J.D., Surdam, R.C., 1986. Organic-inorganic interactions as a mechanism for porosity enhancement in the upper cretaceous Ericson sandstone, Green River basin, Wyoming. *Roles of Organic Matter in Sediment Diagenesis* 38–109.
- Fang, Z., 2002. Hydrocarbon exploration significance of intersalt sediments in Qianjiang saline lake basin (in Chinese). *Acta Sedimentol. Sin.* 20, 608–613.
- Feng, Y., Zhang, Y., Wang, R., Zhang, G., Wu, W., 2011. Dolomites genesis and hydrocarbon enrichment of the Fengcheng Formation in the northwestern margin of Junggar Basin. *Petrol. Explor. Dev.* 38, 685–692.
- Fernandez-Turiel, J.L., Garcia-Valles, M., Gimeno-Torrente, D., Saavedra-Alonso, J., Martinez-Manent, S., 2005. The hot spring and geyser sinters of El Tatio, Northern Chile. *Sediment. Geol.* 180, 125–147.
- Fouke, B.W., 2011. Hot-spring systems geobiology: abiotic and biotic influences on travertine formation at mammoth hot springs, Yellowstone national Park, USA. *Sedimentology* 58, 170–219.
- Gao, J., Liu, J., Ni, Y., 2018. Gas generation and its isotope composition during coal pyrolysis: the catalytic effect of nickel and magnetite. *Fuel* 222, 74–82.
- Handley, K.M., Campbell, K.A., Mountain, B.W., Browne, P.R.L., 2005. Abiotic-biotic controls on the origin and development of spicular sinter: in situ growth experiments, Champagne Pool, Waiotapu, New Zealand. *Geobiology* 3, 93–114.
- Heap, M.J., Baud, P., Reuschlé, T., Meredith, P.G., 2014. Stylolites in limestones: barriers to fluid flow? *Geology* 42, 51–54.
- Hu, T., Pang, X., Yu, S., Wang, X., Pang, H., Guo, J., Jiang, F., Shen, W., Wang, Q., Xu, J., 2016. Hydrocarbon generation and expulsion characteristics of Lower Permian P1f source rocks in the Fengcheng area, northwest margin, Junggar Basin, NW China: implications for tight oil accumulation potential assessment. *Geol. J.* 51, 880–900.
- Hu, T., Pang, X., Yu, S., Yang, H., Wang, X., Pang, H., Guo, J., Shen, W., Xu, J., 2017. Hydrocarbon generation and expulsion characteristics of P1f source rocks and tight oil accumulation potential of Fengcheng area on northwest margin of Junggar Basin, Northwest China (in Chinese). *J. Cent. S. Univ.* 48, 427–439.
- Huang, D.F., Li, J.C., Zhou, Z.H., Gu, X.Z., Zhang, D.J., 1984. Evolution and Hydrocarbon Generation Mechanisms of Terrestrial Organic Matter. Petroleum Industry Press, Beijing (in Chinese).
- Huang, P., Ren, J., Li, E., Ma, W., Xu, H., Yu, S., Zou, Y., Pan, C., 2016. Biomarker and carbon isotopic compositions of source rock extracts and crude oils from Mahu Sag, Junggar Basin (in Chinese). *Geochimica* 45, 303–314.
- Jagniecki, E.A., Lowenstein, T.K., 2015. Evaporites of the Green River formation, bridger and piceance Creek basins: deposition, diagenesis, paleobrine chemistry, and Eocene atmospheric CO<sub>2</sub>. In: *Stratigraphy and Paleolimnology of the Green River Formation*. Springer Netherlands, Western USA, pp. 277–312.
- Jahnke, L.L., Embaye, T., Hope, J., Turk, K.A., Van Zuilen, M., Des Marais, D.J., Farmer, J.D., Summons, R.E., 2004. Lipid biomarker and carbon isotopic signatures for stromatolite-forming, microbial mat communities and *Phormidium* cultures from Yellowstone National Park. *Geobiology* 2, 31–47.
- Jiang, Y., Wen, H., Qi, L., Zhang, X., Li, Y., 2012. Salt minerals and their genesis of the permian Fengcheng Formation in Urho area, Junggar Basin (in Chinese). *J. Mineral. Petrol.* 32, 105–114.
- Jin, Q., Wang, J., Song, G., Wang, L., Lin, L., Bai, S., 2010. Interaction between source rock and evaporite: a case study of natural gas generation in the northern Dongying Depression. *Chin. J. Geochem.* 29, 75–81.
- Johnson, R.C., Birdwell, J.E., Mercier, T.J., Brownfield, M.E., Charpentier, R.R., Klett, T.R., Leathers, H.M., Schenk, C.J., Tennyson, M.E., 2015. Assessment of Undiscovered Oil and Gas Resources in the Uteland Butte Member of the Eocene Green River Formation, Uinta Basin, Utah. U.S. Geological Survey Fact Sheet 2015-3052, 2p.
- Johnson, R.C., Mercier, T.J., Brownfield, M.E., 2014. Spatial and Stratigraphic Distribution of Water in Oil Shale of the Green River Formation Using Fischer Assay, Piceance Basin, Northwestern Colorado. *Environmental Geology of Oil Shale & Tar Sands*.
- Jones, B., Peng, X., 2016. Mineralogical, crystallographic, and isotopic constraints on the precipitation of aragonite and calcite at Shiqiang and other hot springs in Yunnan Province, China. *Sediment. Geol.* 345, 103–125.
- King, S.A., Behnke, S., Slack, K., Krabbenhoft, D.P., Nordstrom, D.K., Burr, M.D., Striegl, R.G., 2006. Mercury in water and biomass of microbial communities in hot springs of Yellowstone National Park, USA. *Appl. Geochem.* 21, 1868–1879.
- Koehn, D., Renard, F., Toussaint, R., Paschier, C., 2007. Growth of stylolite teeth patterns depending on normal stress and finite compaction. *Earth Planet Sci. Lett.* 257, 582–595.
- Koehn, D., Rood, M.P., Beaudoin, N., Chung, P., Bons, P.D., Gomez-Rivas, E., 2016. A new stylolite classification scheme to estimate compaction and local permeability variations. *Sediment. Geol.* 346, 60–71.
- Kuang, L., Tang, Y., Lei, D., Chang, Q., Ouyang, M., Hou, L., Liu, D., 2012. Formation conditions and exploration potential of tight oil in the Permian saline lacustrine dolomitic rock, Junggar Basin, NW China. *Petrol. Explor. Dev.* 39, 700–711.
- Lalonde, S.V., Amskold, L., McDermott, T.R., Inskip, W.P., Konhauser, K.O., 2007. Chemical reactivity of microbe and mineral surfaces in hydrous ferric oxide depositing hydrothermal springs. *Geobiology* 5, 219–234.
- Liang, C., Cao, Y., Jiang, Z., Wu, J., Guoqi, S., Wang, Y., 2017. Shale oil potential of lacustrine black shale in the Eocene Dongying depression: implications for geochemistry and reservoir characteristics. *AAPG (Am. Assoc. Pet. Geol.) Bull.* 101, 1835–1858.
- Liang, C., Jiang, Z., Cao, Y., Jing, W., Wang, Y., Fang, H., 2018. Sedimentary characteristics and origin of lacustrine organic-rich shale in the salinized Eocene Dongying Depression. *Geol. Soc. Am. Bull.* 130, 154–174.
- Liu, B., Liu, D., Guo, T., Huang, Z., Liu, Z., Wu, F., 2013. Oil accumulation related to migration of source kitchens in northwestern margin structural belt, Junggar Basin (in Chinese). *Petroleum Geology & Experiment* 35, 621–625.
- Liu, G.D., Chen, Z.L., Wang, X.L., Gao, G., Xiang, B.L., Ren, J.L., Ma, W.Y., 2016. Migration and accumulation of crude oils from Permian lacustrine source rocks to Triassic reservoirs in the Mahu depression of Junggar Basin, NW China: constraints from pyrrolic nitrogen compounds and fluid inclusion analysis. *Org. Geochem.* 101, 82–98.
- Lu, X., Zhang, S., Shi, J., 2012. Dolomite genesis and geochemical characteristics of permian Fengcheng Formation in Weerhe-Fengcheng area, northwestern Junggar basin (in Chinese). *J. Lanzhou Univ.* 48, 8–20.
- Luo, Q., George, S.C., Xu, Y., Zhong, N., 2016. Organic geochemical characteristics of the Mesoproterozoic Hongshuizhuang Formation from northern China: implications for thermal maturity and biological sources. *Org. Geochem.* 99, 23–37.
- Luo, Q., Hao, J., Skovsted, C.B., Luo, P., Khan, I., Wu, J., Zhong, N., 2017. The organic petrology of graptolites and maturity assessment of the Wufeng-Longmaxi Formations from Chongqing, China: insights from reflectance cross-plot analysis. *Int. J. Coal Geol.* 183, 161–173.
- Luo, Q., Gong, L., Qu, Y., Qu, Y., Zhang, K., Zhang, G., Wang, S., 2018a. The tight oil potential of the Lucaogou Formation from the southern Junggar Basin, China. *Fuel* 234, 858–871.
- Luo, Q., Zhong, N., Liu, Y., Qu, Y., Ma, L., 2018b. Organic geochemical characteristics and accumulation of the organic matter in the jurassic to cretaceous sediments of the saihantala sag, erlian basin, China. *Mar. Petrol. Geol.* 92, 855–867.
- Ma, C., Elsworth, D., Dong, C., Lin, C., Luan, G., Chen, B., Liu, X., Muhammad, J.M., Muhammad, A.Z., Shen, Z., Tian, F., 2017. Controls of hydrocarbon generation on the development of expulsion fractures in organic-rich shale: based on the paleogene shahejie Formation in the jiyang depression, bohai bay basin, east China. *Mar. Petrol. Geol.* 86, 1406–1416.
- Ma, D., He, D., Li, D., Tang, J., Liu, Z., 2015. Kinematics of syn-tectonic unconformities and implications for the tectonic evolution of the hala'alat Mountains at the northwestern margin of the Junggar Basin, central asian orogenic belt. *Geoscience Frontiers* 6, 247–264.
- Ma, S., Xia, Y., Tian, C., Yang, Y., 2013. Elemental geochemical indicators for sedimentary environment in lacustrine carbonate source rocks of the Biyang depression, Nanxiang Basin (in Chinese). *Bull. China Soc. Mineral Petrol. Geochem.* 32, 456–462.
- Ma, X., Zheng, G., Sajjad, W., Xu, W., Fan, Q., Zheng, J., Xia, Y., 2018. Influence of minerals and iron on natural gases generation during pyrolysis of type-III kerogen. *Mar. Petrol. Geol.* 89, 216–224.
- Ma, X., Zheng, J., Zheng, G., Xu, W., Qian, Y., Xia, Y., Wang, Z., Wang, X., Ye, X., 2016a. Influence of pyrite on hydrocarbon generation during pyrolysis of type-III kerogen. *Fuel* 167, 329–336.
- Ma, Y., Fan, M., Lu, Y., Liu, H., Hao, Y., Xie, Z., Liu, Z., Peng, L., Du, X., Hu, H., 2016b. Climate-driven paleolimnological change controls lacustrine mudstone depositional process and organic matter accumulation: constraints from lithofacies and geochemical studies in the Zhanhua Depression, eastern China. *Int. J. Coal Geol.* 167, 103–118.
- MacGowan, D.B., Surdam, R.C., 1990. Importance of Organic—Inorganic Reactions to

- Modeling Water—rock Interactions during Progressive Clastic Diagenesis. ACS Publications.
- Martín-Martín, J.D., Gomez-Rivas, E., Gómez-Gras, D., Travé, A., Ameneiro, R., Koehn, D., Bons, P.D., 2017. Activation of stylolites as conduits for overpressured fluid flow in dolomitized platform carbonates. *Geol. Soc. London Spec. Publ.* 459 SP459. 3.
- Mercier, T.J., 2012. Isopach and Isoresource Maps for Oil Shale Deposits in the Eocene Green River Formation for the Combined Uinta and Piceance Basins, Utah and Colorado. Center for Integrated Data Analytics Wisconsin Science Center.
- Mileshina, A.G., Moskalev, N.P., 1962. Stylolites in Limestones as Paths of Migration of Oil.
- Norman, K., 2015. Stylolitization of Limestone: a Study about the Morphology of Stylolites and its Impacts of Porosity and Permeability in Limestone.
- Olcott, M.A., Cestari, N.A., 2015. Biomarker analysis of samples visually identified as microbial in the Eocene Green River formation: an analogue for mars. *Astrobiology* 15, 770–775.
- Osburn, M.R., Sessions, A.L., Pepe-Ranney, C., Spear, J.R., 2011. Hydrogen-isotopic variability in fatty acids from Yellowstone National Park hot spring microbial communities. *Geochem. Cosmochim. Acta* 75, 4830–4845.
- Ougier-Simonin, A., Renard, F., Boehm, C., Vidal-Gilbert, S., 2016. Microfracturing and microporosity in shales. *Earth Sci. Rev.* 162, 198–226.
- Pan, C., Jiang, L., Liu, J., Zhang, S., Zhu, G., 2010. The effects of calcite and montmorillonite on oil cracking in confined pyrolysis experiments. *Org. Geochem.* 41, 611–626.
- Park, W.C., Schot, E.H., 1968. Stylolites: their nature and origin. *J. Sediment. Res.* 38, 175–191.
- Peters, K.E., Walters, C.C., Moldowan, J.M., 2005. *The Biomarker Guide*. Cambridge University Press.
- Prieto-Barajas, C.M., Alfaro-Cuevas, R., Valencia-Cantero, E., Santoyo, G., 2017. Effect of seasonality and physicochemical parameters on bacterial communities in two hot spring microbial mats from Araró, Mexico. *Rev. Mex. Biodivers.* 88, 616–624.
- Rahman, H.M., Kennedy, M., Löhr, S., Dewhurst, D.N., 2017. Clay-organic association as a control on hydrocarbon generation in shale. *Org. Geochem.* 105, 42–55.
- Rahman, H.M., Kennedy, M., Löhr, S., Dewhurst, D.N., Sherwood, N., Yang, S., Horsfield, B., 2018. The influence of shale depositional fabric on the kinetics of hydrocarbon generation through control of mineral surface contact area on clay catalysis. *Geochem. Cosmochim. Acta* 220, 429–448.
- Ramos, J.R.D.A., 2001. Stylolites: measurement of rock loss. *Rev. Bras. Geociencias* 30, 432–435.
- Ren, J., Jin, J., Wang, M., Dilidaer, R., Li, J., 2017. Analysis of hydrocarbon potential of lower permian in Mahu sag, Junggar Basin (in Chinese). *Geol. Rev.* 63, 51–52.
- Renaut, R.W., Jones, B., Tiercelin, J.J., 1998. Rapid in situ silicification of microbes at Loburu hot springs, Lake Bogoria, Kenya Rift Valley. *Sedimentology* 45, 1083–1103.
- Roeselers, G., Norris, T.B., Castenholz, R.W., Rysgaard, S., Glud, R.N., Kühl, M., Muyzer, G., 2007. Diversity of phototrophic bacteria in microbial mats from Arctic hot springs (Greenland). *Environ. Microbiol.* 9, 26–38.
- Schieber, J., 1999. Microbial mats in terrigenous clastics; the challenge of identification in the rock record. *Palaios* 14, 3–12.
- Schieber, J., Bose, P.K., Eriksson, P.G., Banerjee, S., Sarkar, S., Altermann, W., Catuneanu, O., 2007. *Atlas of Microbial Mat Features Preserved within the Siliciclastic Rock Record*. Elsevier.
- Schulz, H.M., Schovsbo, N., Wirth, R., Schreiber, A., van Berk, W., 2017. Organic-inorganic interactions during reactive fluid flow in carbonates. In: *Eage Workshop on Evaluation and Drilling of Carbonate Reservoirs*.
- Schulz, H.M., Wirth, R., Schreiber, A., 2016. Organic-inorganic rock-fluid interactions in stylolitic micro-environments of carbonate rocks: a FIB-TEM study combined with a hydrogeochemical modelling approach. *Geofluids* 16, 909–924.
- Seewald, J.S., 2003. Organic-inorganic interactions in petroleum-producing sedimentary basins. *Nature* 426, 327–333.
- Shi, C., Bao, Z., Zhang, J., Ding, F., 2015. Sedimentary characteristics of braided stream—braided fan of Shawan Formation in Chunfeng Oilfield, northwest margin of Junggar Basin, China. *Arabian Journal of Geosciences* 8, 4469–4484.
- Siljeström, S., Parenteau, M.N., Jahnke, L.L., Cady, S.L., 2017. A comparative ToF-SIMS and GC-MS analysis of phototrophic communities collected from an alkaline silica-depositing hot spring. *Org. Geochem.* 109, 14–30.
- Suárez-Ruiz, I., Flores, D., Filho, J.G.M., Hackley, P.C., 2012a. Review and update of the applications of organic petrology: Part 2, geological and multidisciplinary applications. *Int. J. Coal Geol.* 98, 73–94.
- Suárez-Ruiz, I., Flores, D., Mendonça Filho, J.G., Hackley, P.C., 2012b. Review and update of the applications of organic petrology: Part 1, geological applications. *Int. J. Coal Geol.* 99, 54–112.
- Surdam, R.C., Wolfbauer, C.A., 1973. Origin of Oil Shale in the Green River Formation (Wyoming).
- Talbot, M.R., 1988. The origins of lacustrine oil source rocks: evidence from the lakes of tropical Africa. *Geological Society* 40, 29–43.
- Tänavstuu-Milkeviciene, K., Sarg, J.F., 2012. Evolution of an organic-rich lake basin - stratigraphy, climate and tectonics: Piceance Creek basin, Eocene Green River Formation. *Sedimentology* 59, 1735–1768.
- Tao, K.Y., Cao, J., Wang, Y.C., Ma, W.Y., Xiang, B.L., Ren, J.L., Zhou, N., 2016. Geochemistry and origin of natural gas in the petroliferous Mahu sag, northwestern Junggar Basin, NW China: Carboniferous marine and Permian lacustrine gas systems. *Org. Geochem.* 100, 62–79.
- Teixeira, M.G., Donzé, F., Renard, F., Panahi, H., Papachristos, E., Scholtès, L., 2017. Microfracturing during primary migration in shales. *Tectonophysics* 694, 268–279.
- Tissot, B.P., Welte, D.H., 1984a. *Oil and Source Rock Correlation*. Springer Berlin Heidelberg, pp. 472–486.
- Tissot, B.P., Welte, D.H., 1984b. *Petroleum Formation and Occurrence*. Springer-Verlag, pp. 643–644.
- Tuo, J., Zeng, F., Huang, X., Ma, W., 1997. Biyang depression-an example of lacustrine carbonate as source rocks of petroleum (in Chinese). *Acta Sedimentol. Sin.* 15, 64–69.
- Wang, J., 2009. A Study on Interaction of Source Rock and Oil with Evaporates in Saline-Lake Facies (In Chinese). China University of Petroleum, East China, pp. 101.
- Wang, M., 2017. Minerals of the lower permian Fengcheng Formation in Mahu sag, Junggar Basin and their indicating significance (in Chinese). *Geol. Rev.* 63, 305–306.
- Wang, Q., Gao, P., Zhu, S., Li, C., 1983. Sedimentary environment and characteristics of parent oil-forming matter and reservoir rock of Biyang depression (in Chinese). *Earth Science-Journal of Wuhan College of Geology* 20, 135–146.
- Wang, S.Z., Zhang, K.H., Jin, Q., 2014. The genetic types of crude oils and the petroleum geological significance of the Fengcheng Formation source rock in hashan area, Junggar Basin (in Chinese). *Natural Gas Geoscience* 25, 595–602.
- Warren, J.K., 2006. *Evaporites Sediments, Resources and Hydrocarbons*. Springer, pp. 1–1035.
- Warren, J.K., 2010. Evaporites through time: tectonic, climatic and eustatic controls in marine and nonmarine deposits. *Earth Sci. Rev.* 98, 217–268.
- Xiao, F., Liu, L., Zhang, Z., Wu, K., Xu, Z., Zhou, C., 2014. Conflicting sterane and aromatic maturity parameters in Neogene light oils, eastern Chepaizi High, Junggar Basin, NW China. *Org. Geochem.* 76, 48–61.
- Yang, Z., Tong, R., Fan, Z., 1983. Biological mark compounds of source rocks and crude oil from Jianghan salt basin and their geological significance. *Oil Gas Geol.* 39–52.
- Yu, K., Cao, Y., Qiu, L., Sun, P., Yang, Y., Qu, C., Wan, M., 2016a. Characteristics of alkaline layer cycles and origin of the lower permian Fengcheng Formation in Mahu sag, Junggar Basin (in Chinese). *J. Palaeogeogr.* 18, 1012–1029.
- Yu, K., Cao, Y., Qiu, L., Sun, P., Yang, Y., Qu, C., Li, Y., Wan, M., Su, Y., 2016b. Brine evolution of ancient lake and mechanism of carbonate minerals during the sedimentation of early permian Fengcheng Formation in Mahu depression, Junggar Basin, China (in Chinese). *Natural Gas Geoscience* 27, 1248–1263.
- Zhang, C.L., Fouke, B.W., Bonheyo, G.T., Peacock, A.D., White, D.C., Huang, Y., Romanek, C.S., 2004. Lipid biomarkers and carbon-isotopes of modern travertine deposits (Yellowstone National Park, USA): implications for biogeochemical dynamics in hot-spring systems. *Geochem. Cosmochim. Acta* 68, 3157–3169.
- Zhang, J., He, Z., Xu, H., Ji, H., Yuan, Q., Shi, J., Lu, X., 2012. Petrological characteristics and origin of permian Fengcheng Formation dolomitic rocks in wuerhe-fengcheng area, Junggar Basin (in Chinese). *Acta Sedimentol. Sin.* 30, 859–867.
- Zhang, Y., Wang, G., Yang, Y., Qi, Z., 2005. Rhythms of saline lake sediments of the Paleogene and their paleoclimatic significance in Qianjiang Sag, Jianghan Basin (in Chinese). *J. Palaeogeogr.* 7, 461–470.
- Zhong, J., Kong, F., Li, Y., Yuan, X., Gao, Y., Liang, G., Ahmatjan, A.R., Chen, X., Niu, Y., Wang, P., 2010. Research of stylolites in ordovician carbonate reservoirs of the 4th block, tahe Oilfield, Tarim basin (in Chinese). *Geol. Rev.* 56, 841–850.
- Zhou, Z., Dong, Q., Hou, G., Xu, S., Miao, C., 2006. The forming environment and sedimentary evolution of oil shale intergrowing with salt alkali mine- with the oil shale deposit of wucheng, Tongbai Basin as an example (in Chinese). *J. Jilin Univ. (Earth Sci. Ed.)* 36, 1001–1005.
- Zhu, S., Xian, B., Zhu, X., Liu, J., Yuan, Y., Niu, H., Zhao, C., 2012a. Genesis and hydrocarbon significance of vesicular welded tuffs: a case study from the Fengcheng Formation, Wu-Xia area, Junggar Basin, NW China. *Petrol. Explor. Dev.* 39, 173–183.
- Zhu, S., Zhu, X., Niu, H., Han, X., Zhang, Y., 2012b. Genetic mechanism of dolomitization in Fengcheng Formation in the Wu-Xia area of Junggar Basin, China. *Acta Geologica Sinica-English Edition* 86, 447–461.
- Zhu, S.F., Zhu, X.M., Liu, X., Wu, D., Zhao, D.N., 2016. Authigenic minerals and diagenetic evolution in altered volcanic materials and their impacts on hydrocarbon reservoirs: evidence from the lower Permian in the northwestern margin of Junggar Basin, China. *Arabian Journal of Geosciences* 9, 97.
- Zhu, S.F., Zhu, X.M., Tao, W.F., Liu, S.Q., Chen, H.H., Zhang, Y.Q., 2013. Origin of dolomitic reservoir rock in the permian Fengcheng Formation in WuXia area of the Junggar Basin. *Geol. J. China Univ.* 19, 38–45.